CO_2 hydrogenation for the production of higher alcohols
Trends in catalyst developments, challenges and opportunities

Latsiou, Angeliki I.; Charisiou, Nikolaos D.; Frontistis, Zacharias; Bansode, Atul; Goula, Maria A.

DOI
10.1016/j.cattod.2023.114179

Publication date
2023

Document Version
Final published version

Published in
Catalysis Today

Citation (APA)
Latsiou, A. I., Charisiou, N. D., Frontistis, Z., Bansode, A., & Goula, M. A. (2023). CO_2 hydrogenation for the production of higher alcohols: Trends in catalyst developments, challenges and opportunities. *Catalysis Today*, *420*, Article 114179. https://doi.org/10.1016/j.cattod.2023.114179

Catalysis Today 420 (2023) 114179

Contents lists available at ScienceDirect

Catalysis Today

journal homepage: www.elsevier.com/locate/cattod

CO_2 hydrogenation for the production of higher alcohols: Trends in catalyst developments, challenges and opportunities

Angeliki I. Latsiou [a], Nikolaos D. Charisiou [a], Zacharias Frontistis [b], Atul Bansode [c], Maria A. Goula [a,*]

[a] Laboratory of Alternative Fuels and Environmental Catalysis (LAFEC), Department of Chemical Engineering, University of Western Macedonia, GR-50100, Greece
[b] Department of Chemical Engineering, University of Western Macedonia, GR-50100, Greece
[c] Department of Chemical Engineering, Delft University of Technology, Van der Massweg 9, 2629 Hz Delft, the Netherlands

ARTICLE INFO

Keywords:
CO_2 hydrogenation
Higher alcohol production
Heterogeneous catalyst developments
Promoters & supports effect
Thermodynamic analysis
Reaction mechanism

ABSTRACT

Higher alcohol (HA) synthesis via the hydrogenation of CO_2 constitutes a relatively new and exciting field of research that has the potential to help towards the de-carbonization of the energy sector. The process poses formidable challenges, as it demands the formation of at least one C-C bond, when CO_2 is thermodynamically stable, fully oxidized and kinetically inert. This work provides a comprehensive and critical literature review of the catalytic formulations that have been employed, in both fixed-bed and batch reactors, which include noble metal catalysts, transition metal-based systems, post-transition metal catalysts, bimetallic, multimetallic/multi-functional catalysts, Metal Organic Frameworks (MOFs), perovskite-, and zeolite-based catalysts. The critical role of promoters and supports and the effect that the reaction conditions have on performance are also discussed. Emphasis has been given to single atom catalysts (SACs), as the high specific activity of these systems seems to hold great promise for the reaction at hand. Breakthroughs made by employing the concept of tandem catalysis are also critically analyzed. This review paper also discusses the thermodynamic aspects of the reaction and the insights that have been gained regarding the reaction mechanism. Finally, it provides an overview of the direction that research may move to into the future.

1. Introduction

The foundation for the economic growth that the world has gone through since the industrial age has been provided by fossil fuels. However, as is now well understood, the emission of greenhouse gases during their combustion and the subsequent increase in their atmospheric concentration, is causing visible changes in global climate everywhere in the world. The increase in the concentration of carbon dioxide (CO_2) in the atmosphere has jumped from a long-term mean average of 275 ppm in the pre-industrial epoch, to 340 in the 1980's, to the current level of about 420 ppm [1]. Although the effects of climate change are fast becoming the familiar horsemen of a planetary apocalypse, results from climate model simulations indicate that our planet's average temperature will rise from 1.1° to 5.4°C in 2100 [2].

As the world is working towards de-carbonizing the energy sector, it is imperative that in the meantime efforts are made to not only curb, capture or store CO_2 emissions, but also of finding ways to utilize them. In this direction, efforts are intensifying and include the conversion of CO_2 via hydrogenation into valuable products such as carbon monoxide (CO) [3–5], light olefins (C_nH_{2n}) [6–10], hydrocarbons (HC) [11–17], formic acid (HCOOH) [18–21], formaldehyde (HCHO) [22], dimethyl ether (DME) [23–26], methanol (CH_3OH) [27–30] and higher alcohols ($C_{2+}OH$) [31–36].

Among the aforementioned products, the synthesis of higher alcohols (HAs) constitutes a relatively new area of research, but recent geopolitical conflicts, which has plugged the chemical sector into uncertainty and caused the price of gasoline and natural gas to skyrocket, has made abundantly clear that the production of chemicals deserves additional impetus. At present, the focus of the scientific community is on the use of higher alcohols as alternative fuel additives, as they are known to offer a plethora of advantages, in comparison to for example, methanol, which has been extensively studied. In particular, higher alcohols are less toxic, have lower volatility, better solubility in fuel and a higher energy density. Moreover, their higher-octane number leads to a

---

* Correspondence to: University of Western Macedonia, Department of Chemical Engineering, Laboratory of Alternative Fuels and Environmental Catalysis, ZEP, Kozani 50100, Greece.
E-mail address: mgoula@uowm.gr (M.A. Goula).

https://doi.org/10.1016/j.cattod.2023.114179
Received 19 January 2023; Received in revised form 11 April 2023; Accepted 6 May 2023
Available online 8 May 2023
0920-5861/

reduction in the emission of noxious gases (NO_x, O_3, CO, and VOCs) during their combustion [37,38]. For instance, it has been reported that the use of a fuel composed of 10% ethanol and 90% gasoline in internal combustion engines (ICEs) leads to a decline of CO emissions by 30% [39,40]. Higher alcohols can also be used to produce value-added chemicals such as olefins (which could be produced from ethanol and butanol via dehydration) and methyltertiarybutylether (MTBE) [41]. Moreover, higher alcohols can also be used as alternative energy carriers in fuel cells technologies [42]. Thus, due to their economic value and their broad range of industrial applications, higher alcohols are a very promising feedstock that can help pave the way for the sustainable development of future energy systems and the manufacture of chemicals [43].

Nowadays, $C_{2–4}$ alcohols are mainly synthesized through the following routes: (i) fermentation of carbon-based agricultural feedstocks (corn and sugarcane, glucose (sugar), starch, ligno-celluloses) [44,45], (ii) hydration of petroleum-derived alkenes [46–48], and (iii) hydrogenation of CO (syngas) [49–53]. However, there are a number of disadvantages associated with the above-mentioned processes. To start with, the fermentation route, which has been already commercialized, raises serious ethical questions (food versus fuel), as it demands the use of edible plants (e.g., corn and sugarcane), it is an energy-demanding process, and offers a rather low product yield [31]. Concerning the hydration route, its use not only intensifies our dependence on crude oil, but the process also suffers from low conversions and poor catalyst stability [54]. Finally, the process where syngas mixtures (CO and H_2), derived from reforming or partial oxidation of coal, natural gas, or biomass, that are then hydrogenated to HAs, does not appear capable of meeting the overall market demand [42]. Thus, finding new, sustainable methods based on renewable feedstocks for the production of higher alcohols is a challenge worthy of pursuit.

As an alternative, CO_2 a nontoxic and renewable carbon source could be a promising candidate, replacing CO, for higher alcohols production and making possible both the simultaneous abatement of CO_2 emissions and its effective exploitation. However, its activation and transformation are not easy to accomplish as CO_2 is thermodynamically stable (its bond-dissociation energy is 526 kJ mol^{-1}), fully oxidized and kinetically inert [34,54]. Therefore, its transformation to chemicals is a huge scientific challenge, necessitating the presence of a high energy molecule, such as H_2, which can promote CO_2 conversion making feasible its activation and dissociation [55]. However, caution is needed as a high hydrogen to carbon ratio results in C1 products (CO, CH_3OH, CH_4) due to the rapid hydrogenation of reaction intermediates [56]. Moreover, the success of C-C bond formation poses another formidable challenge, as HAs consists of one C-O bond and at least one C-C bond. Therefore, an effective catalyst should promote both CO_2 activation and C-C coupling on its surface [57]. Until now, although great efforts have been expended to design and synthesize selective catalytic systems, there is still the need for further investigation and improvement prior to industrial use.

Given the increased research interest in the reaction of CO_2 hydrogenation for the production of higher alcohols witnessed in the last few years, some high-quality review papers have already been published [31–36]; the caveat is that such reports are still few compared to the existing reviews concerning the conversion of CO_2 to methanol [e.g., 58, 59], hydrocarbons [e.g., 60,61] or syngas [e.g., 62,63]. In one of the earliest efforts, Schemme et al. [36] reviewed the maturity of the technologies used to synthesize C_1-C_8 alcohols. Both Gao et al. [33] and Zhang et al. [34] provided review papers dealing with the production of liquid fuels from CO_2 hydrogenation, i.e., the focus of these works was not exclusively on higher alcohols synthesis. Another effort was carried out by Liu at al. [35] who focused solely on hetero-site cobalt catalysts, an important family of catalytic systems, for the synthesis of higher alcohols via CO_2 hydrogenation. The most recent review papers, dealing with advances in CO_2 hydrogenation to HAs in terms of catalyst design and performance, as well as information into the reaction mechanism, have been provided by Zeng et al. [31] and Xu et al. [32].

Herein, we have attempted to provide a comprehensive and critical literature review of the catalytic formulations that have been employed, in both fixed-bed and batch reactors, which include noble metal catalysts (e.g., Rh, Pd, Au), transition-based systems (e.g., Fe, Mo, Co, Cu), post-transition catalysts, bimetallic, multimetallic/multifunctional catalysts, Metal Organic Frameworks (MOFs), perovskite-, and zeolite-based catalysts, to tackle the complexities and formidable challenges that this reaction poses. The critical role of promoters (for example, alkali metals are almost indispensable in the majority of catalytic systems employed) and supports (such as the role of oxygen vacancies and of oxygen lability, metal-support interactions) and the effect that the reaction conditions (including the role of solvents in the works employing batch reactors) have on performance are also discussed. Particular emphasis has been given to single atom catalysts (SACs), as the high specific activity of these systems seems to hold great promise for the reaction at hand. Breakthroughs made by employing the concept of tandem catalysis are also critically analyzed. This review paper also discusses the thermodynamic aspects of the reaction and the insights that have been gained regarding the reaction mechanism. Finally, it provides an overview of the direction that research may move to into the future.

2. Thermodynamics analysis

Although there exist numerous reports in the literature that have presented thermodynamic analysis for the hydrogenation of CO_2 to methane or methanol [57,64–67], the relatively recent focus of the scientific community to the production of HAs means that only few have investigated the thermodynamics of this reaction [57,68–70]. That being said, it is generally thought that HAs synthesis proceeds through the Reverse Water Gas Shift Reaction (RWGS) and the subsequent hydrogenation of CO, as follows [57,68–73]:

Reverse water gas shift reaction: $CO_2 + H_2 \rightarrow CO + H_2O \ \Delta H^{\circ}_{273K} = 41{\cdot}2 \text{ kJ mol}^{-1}$ (1)

Alcohol formation reaction: $nCO + 2nH_2 \rightarrow C_nH_{2n+1}OH + (n - 1)\ H_2O$ (2)

Overall reaction: $nCO_2 + 3nH_2 \leftrightarrow C_nH_{2n+1}OH + (2n\text{-}1)\ H_2O$ (3)

All of the available works have employed the Gibbs free energy minimization method, which is based on the assumption that the system under consideration processes the minimum total Gibbs free energy at equilibrium, meaning that it is not necessary to know the equilibrium constant at each reaction step [68,74]. Jia et al. [68] conducted one of the earliest thermodynamic analysis of CO_2 hydrogenation to ROH, but also for a variety of other products (CO, RCOOH, RCHO, HC). The authors showed that the conversion of CO_2 to products with high number of carbons in their structure (butene, butyne, butanol, propionaldehyde, propionic acid) is favored at low temperature (<200 °C) and high pressure (>10 bar). Moreover, they also showed that the Gibbs free energy (at 25 °C) for the hydrogenation of CO_2 to ethanol, propanol and butanol is – 32.4 kJ mol^{-1}, – 39.9 kJ mol^{-1} and – 43.2 kJ mol^{-1}, respectively, while that for the production of methanol is 3.5 kJ mol^{-1}. Thus, the CO_2 to HAs reaction is more thermodynamically favorable than the corresponding one for methanol production. A comparison between CO_2 conversion to methanol and ethanol at different temperatures and pressures is depicted in Fig. 1(a and b). As can be observed, an increase over a certain reaction temperature leads to a decrease of CO_2 conversion for both methanol and ethanol synthesis due to the exothermic nature of the reaction ($\Delta H^{\Theta} = -49.3$ kJ mol^{-1} and -86.7 kJ mol^{-1}), however this also strongly depends on the reaction pressure. For example, for the synthesis of ethanol, conversion of CO_2 (X_{CO2}) remains close to 100% up to 300 °C at 300 bar. In contrast, X_{CO2} declines even at 150 °C, if the reaction pressure is set at 30 bar. Regarding the product distribution Fig. 1(c and d), the authors concluded that irrespective of

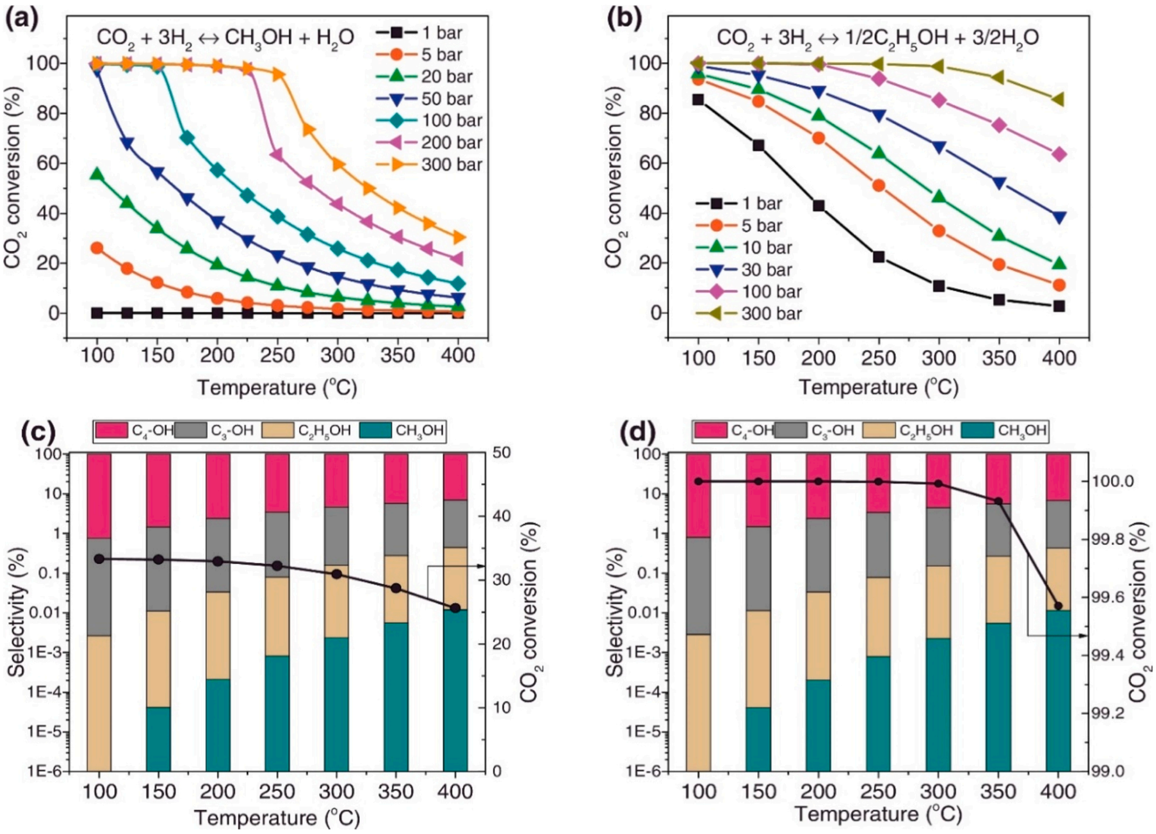

Fig. 1. **(a)** Equilibrium values for CO_2 hydrogenation to methanol, **(b)** Equilibrium values for CO_2 hydrogenation to ethanol, **(c)** Alcohol distribution in the product's mixture at $H_2/CO_2 = 1$ (P = 50 bar), and **(d)** Alcohol distribution in the product's mixture at $H_2/CO_2 = 5$ (P = 200 bar) [68].

the H_2/CO_2 ratio used (1 or 5), at lower temperatures, the formation of butanol is favored.

In a subsequent work He et al. [69] included in the calculations the presence of CH_4 in the products mixture, which thermodynamically is the most favored product, and thus hinders the formation of alcohols. The authors confirmed that the production of HAs benefits from increased pressures and H_2:CO_2 ratio (up to a ratio equal to 3.5–4), while an increase in the reaction temperature leads to an increase in the selectivity to CO, and over approximately 250 °C, also to a decrease in the conversion of CO_2 and H_2. Stangeland et al. [70] took into account the condensation reactions and concluded that these may prove advantageous during CO_2 hydrogenation to higher alcohols. The authors were able to show that when methanol is produced as an intermediate, two molecules can combine between them (methanol homologation), and their dehydration can also lead to the production of ethanol. In the most recently published study, He et al. [57] also included in their thermodynamic analysis the effect that different $C_{1–4}$ alkane isomers, alkene isomers and alcohol isomers have on the production of HAs. The authors were able to show that the more favorable thermodynamically alkane isomer is isobutane, for alkene isomers, the more favorable thermodynamically are isobutene, trans-2-butene, cis-2-butene and propene, and of the alcohol isomers, the more favorable thermodynamically are 1/2-propanol and 1/2/iso/tert-butanol. Moreover, this work also confirmed that CH_4 has a negative impact on the production of HAs, which can however be somewhat suppressed at lower reaction temperatures and higher pressures.

3. Catalyst developments

As mentioned above, an effective HAs producing catalyst via CO_2 hydrogenation should promote both CO_2 activation and C-C coupling on its surface. To meet this challenge, great efforts have been expended to design and synthesize selective catalytic systems, which include monometallic noble metal catalysts (e.g., Rh, Pd, Au), transition-based systems (e.g., Fe, Mo, Co, Cu), post-transition catalysts, bimetallic, and multimetallic / multifunctional catalysts, Metal Organic Frameworks (MOFs), perovskite- and zeolite-based catalysts. Breakthroughs have also been made by employing the concept of tandem catalysis. This section critically discusses the aforementioned catalytic formulations and also provides information on the effect of the supports and of the catalyst structure on catalytic performance.

3.1. Noble metal-based catalysts

3.1.1. Rh-based catalysts

One of the earliest works investigating the formation of HAs via CO_2 hydrogenation was carried out in the 1990 s by Kusama et al. [75], using Rh-based catalysts. In this groundbreaking work, the authors examined the influence of a series of approximately 30 additives (Li, Na, K, Mg, Ca, Sr, Ba, Fe, Co, Ni, Ru, Pd, Ir, Pt, Cu, Ag, Ti, V, Mn, Zr, Nb, Mo, Re, Zn, Sn, La, Ce, Sm), with an atomic ratio of Rh:M= 1:1 (5 wt% Rh, M= additive), to the performance of a Rh/SiO_2 catalyst using a fixed-bed reactor (T = 200–260 °C, P = 1–50 bar, H_2:CO_2 = 0.6–9). Although the addition of the promoters was generally found to increase the conversion of CO_2, only Li, Fe, Sr and Ag led to ethanol formation, with S_{EtOH} recorded as 15.5%, 3.2%, 2.5%, and 1.8%, respectively; X_{CO2} was 7.0%, 10.4%, 2.8% and 2.1%, respectively (T = 240 °C, P = 50 bar, H_2:CO_2 = 3:1). Utilizing in-situ FT-IR, the authors suggested that the addition of Li increased the amount of CO intermediates, which then reacted with $^*CH_3$ and formed ethanol. Moreover, using the Rh-Li/SiO_2 catalyst, the authors were also able to show that ethanol formation is favored at an optimum temperature (over which it declines), a low H_2:CO_2 ratio (higher ratios favor the production of hydrocarbons), and higher pressures (as expected by equilibrium).

As mentioned in the previous paragraph, Kusama et al. [75] showed that apart from Li, the use of Fe as promoter also led to the production of ethanol, likely due to the ability of Fe to adjust the different electronic states of Rh. Thus, the same group [76], carried out a subsequent work in which they used an Rh-Fe/SiO_2 catalyst, and focused their investigation on the effect of the Rh:Fe atomic ratio on ethanol production (the atomic Rh:Fe ratios used where 1:0.1, 1:0.3, 1:0.5, 1:1, 1:2, and 1:3). Notably, all experimental conditions were the same as those used in the work above, apart from the reaction temperature which was slightly higher (instead of 240 ^oC, this study reports results at 260 ^oC). Although the authors do not comment on this, this slight increase in the reaction temperature led to drastically different results; at 240 ^oC, and for Rh: Fe= 1:1, the reported results were X_{CO2}= 10.4%, S_{Me}OH= 16%, S_{Et}OH= 3.2%, S_{CO}= 6.8%, S_{CH4}= 73.9% [75]. In contrast, and again for Rh:Fe ratio= 1:1, at 260 ^oC, the reported results were X_{CO2}= 25.1%, S_{Me}OH= 28.5%, S_{Et}OH= 16.2%, S_{CO}= 27.5%, S_{CH4}= 27.6% [76]. Thus, the methanation activity of the catalyst was inhibited, which favored the production of alcohols. In terms of the effect of the Rh:Fe ratio [76], the authors discovered that S_{EtOH} increased with an increase in the Rh:Fe ratio, while X_{CO2} also increased up to a ratio of 1:2; over this, X_{CO2} slightly declined. The authors also estimated the amount of CO adsorbed on Rh, for all Rh:Fe ratios under consideration, and by hypothesizing that the sites onto which the CO is adsorbed are the active catalytic centers, came to the conclusion that the active sites decrease upon the addition of Fe up to the Rh:Fe= 1:1 ratio; upon further addition of Fe the active centers appear to increase. Thus, the authors proposed that the turnover frequency (TOF) of the catalysts increased upon the addition of Fe.

Over a quarter of century later, Goryachev et al. [77] repeated the attempt to determine the optimal Fe to Rh ratio. Towards this goal, the authors synthesized a series of Fe promoted (5–30 wt%) Rh (5 wt%) catalysts supported on SiO_2 and tested them over a fixed-bed reactor ($T = 250\ ^\circ C$, $P = 75$ bar, $H_2:CO_2 = 3:1$). Their findings suggest that the optimal Rh:Fe ratio is 1:4, which differs from the 1:1 previously reported by Kusama et al. [76]. However, ethanol selectivity was rather low (S_{Et}OH= 8 ± 2%), while methane was the major product (S_{CH4}= 80 ± 10%) regardless of the Rh:Fe ratio used. To improve the production of HAs, the authors [77] then added potassium (as K_2CO_3) into the FeRh/SiO_2, as K is known to favor the non-dissociated CO adsorption, preventing thus, the formation of hydrocarbons. The reported results show that the addition of even small amounts of K could stabilize CO intermediate production and lead in a higher rate of CO insertion. The optimal composition was 2 wt% K, 20 wt% Fe, and 5 wt% Rh (2K20Fe5Rh/SiO_2), as it achieved the lowest methanation activity (S_{CH4}= 46%), and the highest EtOH selectivity (15.9%) and CO_2 conversion (18.4%).

Also inspired by the pioneering work of Kusama et al. [75], Yang et al. [78] utilized both Fe and Li as promoters, and tested a RhFeLi (Rh: Fe:Li= 1:1:1) system in a fixed-bed microreactor ($T = 250\ ^\circ C$, $P = 30$ bar, $CO_2:H_2 = 1:3$). The authors utilized TiO_2 nanorods (NR) as supporting material, as this oxide aids the dispersion of Rh nanoparticles (nps) and promotes the creation of high-density hydroxyl groups. The latter, favor the formation of ethanol upon CO insertion, as they protonate the methanol and dissociate it into *CHx (Fig. 2). After testing catalysts with different Rh contents, the authors reported that the 2.5 wt % RhFeLi/TiO_2 NR system was able to achieve an ethanol selectivity of 31% (X_{CO2}= 16%), which is the highest achieved for the Rh-based catalysts discussed in this subsection (see also Table 1). Additionally, they concluded that the incorporation of the dual promoters (Fe and Li) into the Rh-based catalyst had a beneficial effect on both CO_2 conversion and ethanol selectivity.

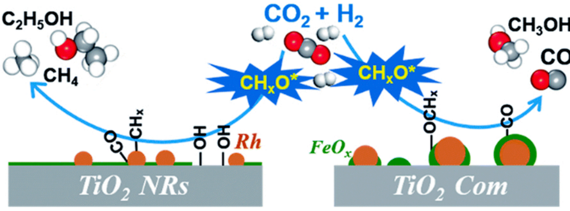

Fig. 2. Schematic representation of the CO_2 hydrogenation over the Rh/TiO_2 with and without hydroxyl groups [78].

In summary, Rh, due to its C-C coupling ability, is a popular noble metal for the production of HAs. However, the addition of alkali or transition metals is necessary to enhance the performance of such systems. For instance, the addition of an alkali metal (Li or K) and/or Fe increases the amount of the CO intermediates, which then reacts with $^*CH_3$ to form ethanol. Moreover, these additives help adjust the different electronic states of Rh. This property is of particular importance, as an electron-rich Rh surface aids the stabilization of $^*CH_3$ and *H species (which in turn inhibits the production of CH_4) promoting the coupling of *CO with $^*CH_3$ to produce the desired HAs. Regarding Fe, caution should be exercised as the existence of Fe^0 leads to the promotion of the undesired methanation reaction, while excess amounts of Fe can also block the Rh active sites. In terms of the supporting material, the use of TiO_2, a material with a high population of oxygen vacancies, has been shown to create high-density hydroxyl groups, which favor the formation of ethanol upon CO insertion, as they protonate the methanol and dissociate it into $^*CH_x$.

3.1.2. *Au-based catalysts*

Although gold has a rich coordination and organometallic chemistry, it was not considered catalytically active until the pioneering works carried out firstly by Bond et al. [79], and then about a decade later, almost simultaneously (but independently), by Haruta [80] and Hutchings [81]. Bond et al. [79] investigated the hydrogenation of olefins, Haruta [80] the low-temperature oxidation of CO, and Hutchings [81] the hydrochlorination of ethyne to vinyl chloride; all concluded that gold-based catalysts showed excellent activity and stability characteristics, and in many cases, were superior to other catalytic systems. Since then, an expanding number of studies have shown that the use of gold-based catalysts leads to exceptional activity and selectivity in various green and sustainable redox reactions and fine chemical synthesis [82–89]. Moreover, an increasing body of published works [e.g., [90–92]] is demonstrating that small Au metal clusters are more reactive in comparison to their bulk analogues, due to the presence of surface atoms that are in low coordination and act as active sites.

Wang et al. [93,94], were the first to investigate the performance of Au nanoclusters (Au NC) for the hydrogenation of CO_2 to ethanol (EtOH). To do so, the authors compared the performance of the Au NC to Pd-, Ir-, and Rh-catalysts supported on TiO_2 ($T = 200\ ^\circ C$, $P = 60$ bar, $CO_2:H_2 = 1:3$), using a batch reactor; the solvent utilized was N, N-dimethylformamide (DMF). The choice of support was inspired by the work carried out by Preti et al. [89], which showed that Au/TiO_2 could be used for the hydrogenation of CO_2 to produce formic acid under high-pressure conditions. Wang et al. [93] demonstrated that the smaller metal particle size (1.0 ± 0.1 nm) and higher dispersion of active species achieved on the Au/TiO_2 (Au= 1.0 wt%) led to an EtOH space time yield (STY) that was higher by an order of magnitude in comparison to the other catalysts (635.4 mmol g^{-1}_{Metal} h^{-1} vs approximately 60 mmol g^{-1}_{Metal} h^{-1}), and more importantly, one of the highest catalytic activity ever reported for EtOH synthesis via this reaction (Tables 1–3). The authors also investigated the effect that different titania polymorphs (anatase, brookite, rutile and amorphous) could have on catalytic activity, this time lowering the loading of the active phase (Au= 0.3 wt%), and reported an even higher EtOH STY (942.8 mmol g^{-1}_{Metal} h^{-1}) for the Au/a-TiO_2 catalyst (Fig. 3a). This improvement was attributed to the enhanced interaction between the Au NC and the a-TiO_2 support, which was the result of the higher population of oxygen vacancies present in this polymorph. Importantly, the as prepared catalyst retained a high S_{EtOH} even after 6 catalytic cycles

Table 1
Composition, synthesis technique, experimental conditions and performance of noble-based catalysts as reported in selected works from the literature.

Catalyst	Synthesis method	Experimental conditions	Catalytic activity	Ref.
5% Rh-Li/SiO_2 (Rh: Li = 1)	Incipient wetness impregnation	fixed-bed reactor, T = 240 °C P = 50 bar, H_2:CO_2 = 3, GHSV= 6000 mL g^{-1} h^{-1}	X_{CO2}= 7.0% $S_{ethanol}$= 15.5%	[75]
5% Rh-Fe/SiO_2 (Rh:Fe = 1:2)	Co-impregnation	fixed-bed reactor, T = 260 °C, P = 50 bar, H_2:CO_2 = 3, GHSV= 6000 mL g^{-1} h^{-1}	X_{CO2}= 26.7% $S_{ethanol}$= 16.0%	[76]
2% K%– 20% Fe-5%Rh/SiO_2 (K: Fe:Rh = 2:20:5)	Wet impregnation	fixed-bed flow-type, T = 250 °C, P = 50 bar, H_2:CO_2 = 3, GHSV= 7000 mL g^{-1} h^{-1}	X_{CO2}= 18.4% $S_{ethanol}$= 15.9% $STY_{Et}OH$= 21.4 $mLg_{cat}^{-1}h^{-1}$	[77]
2.5% RhFeLi/TiO_2 NRs[*1] (Rh/Fe/Li = 1:1:1)	Modified hydrothermal (for the support) and impregnation	fixed-bed reactor, T = 250 ℃ P = 30 bar, H_2:CO_2 = 3, GHSV= 6000 mL g^{-1} h^{-1}	X_{CO2}= 15% $S_{ethanol}$= 32%	[78]
0.3% Au/a-TiO_2 NC[*2]	Deposition−precipitation	batch reactor, T = 200℃ P = 60 bar, H_2: CO_2 = 3, solvent: DMF	X_{CO2}= n/a[*3] $S_{ethanol}$= >99% $STY_{Et}OH$= 942.8 mmol g_{Au}^{-1} h^{-1}	[93]
0.1% Pd/Fe_3O_4 (Pd as single atoms)	Magnetite nanoparticles were functionalized with a $dopPPh_2$ linker by sonication in methanol for 2 h. Pd was loaded from $K_2[PdCl_4]$ to $Fe_3O_4dopPPh_2$ in water, which was followed by reduction with $NaBH_4$.	fixed-bed reactor, T = 250℃ P = 30 bar, H_2:CO_2 = 3, WHSV= 8000 mL g^{-1} h^{-1}	X_{CO2}= 1.4% $S_{ethanol}$= 98% $STY_{Et}OH$= 440 $mmol_{ethanol}$ $g_{Pd}^{-1}h^{-1}$	[98]
0.13% Pd_2/CeO_2 (Pd dimers)	Hydrothermal method (for the support) and adsorption method for the catalyst	fixed-bed reactor, T = 240℃ P = 30 bar, H_2:CO_2 = 3, WHSV= 3000 mL g^{-1} h^{-1}	X_{CO2}= 9.2% $S_{ethanol}$= 99.2% $STY_{Et}OH$= 45.6 $g_{ethanol}$ g_{Pd} $^{-1}$ h^{-1}	[99]
1% Pt/Co_3O_4	Co-precipitation method	batch reactor, T = 200℃, P = 80 bar, H_2:CO_2 = 3, solvent: H_2O-DMI	X_{CO2}= n/a[*3] $STY_{ethanol}$= 29 (100 ×$mmolgcat^{-1}$ h^{-1}) $S_{C2+}OH$= 82.5%	[95]
1% Pt/Co_3O_4-m	Wet impregnation	fixed-bed reactor, T = 200℃, P = 20 bar, H_2:CO_2 = 3, GHSV= 6000 mL g^{-1} h^{-1}	X_{CO2}= ~11% S_ROH= ~48% STY_{HAs}= 1.5 mmol $gcat^{-1}$ h^{-1}	[56]
0.2% Ir_1/In_2O_3 (Ir as single atoms)	Wet impregnation	batch reactor, T = 200℃, P = 60 bar, H_2:CO_2 = 5, solvent: H_2O	X_{CO2}= n/a[*3] $S_{Et}OH$= 99.7% TOF= 481 h^{-1}	[100]

Note: [*1] NR: nanorods, [*2]NC: nanoclusters, [*3] n/a: not available/given

Table 2
Composition, synthesis technique, experimental conditions and performance of transition- and post transition-based metal-catalysts as reported in selected works from the literature.

Catalyst	Synthesis method	Experimental conditions	Catalytic activity	Ref.
K/Cu-Zn-Fe (K:Cu:Zn:Fe= 0.08:1:1:3)	co-precipitation	fixed-bed reactor, T = 300℃, P = 70 bar, H_2:CO_2 = 3, GHSV= 5000 mL g^{-1} h^{-1}	X_{CO2}= 44.2% $S_{ethanol}$= 19.5% $STY_{Et}OH$= ~120 mmol g^{-1} h^{-1}	[102]
$CuZnFe_{0.5}K_{0.15}$ (Cu:Zn:Fe:K= 1:1:0.5:0.15)	co-precipitation and incipient wetness impregnation	fixed-bed reactor, T = 300℃ P = 60 bar, H_2:CO_2 = 3, GHSV= 5000 mL g^{-1} h^{-1}	X_{CO2}= 42.3% S_ROH= 36.67% STY_ROH= 0.17 g/mL h^{-1} $C_{2+}OH/C_1OH$= 6.76	[73]
CoMoS	co-precipitation	fixed-bed reactor, T = 340℃ P = 104 bar, H_2:CO_2 = 3, WHSV= 0.5 kg $kg_{cat}^{-1}h^{-1}$	X_{CO2}= 32% $S_{Et}OH$= 5.5% $S_{Pr}OH$= 0.5% $ROH/C_nH_{2n+2} = 1.58$	[117]
$Mo_1Co_1K_{0.8}$	co-precipitation	fixed-bed reactor, T = 320℃, P = 120 bar, H_2:CO_2 = 3, GHSV= 3000 mL g^{-1} h^{-1}	X_{CO2}= 28.8% $S_{C2+}OH$= 10.9% S_ROH= 81.8%	[37]
$Mo_1Co_{0.3}K_{0.9}$/AC (Mo/activated carbon= 12%)	incipient wetness impregnation	fixed-bed reactor, T = 320℃ P = 50 bar, H_2:CO_2 = 3, GHSV= 3000 mL g^{-1} h^{-1}	X_{CO2}= 23.7% $S_{C2+}OH$= 10.0% S_ROH= 83.2%	[118]
$CoAlO_x$-T (T = 600°C-reduction temperature)	co-precipitation	batch reactor, H_2O solvent, T = 140℃, P = 40 bar, H_2: CO_2 = 3	X_{CO2}= n/a[*1] $S_{Et}OH$= 92.1% STY_ROH= 0.444 mmol $g^{-1}h^{-1}$	[122]
FeNaS (Na= 2.4%, S= 0.6%)	precipitation	fixed-bed reactor, T = 320℃, P = 30 bar, H_2/CO_2 = 3, GHSV = 8000 mL g^{-1} h^{-1}	X_{CO2}= 32.0% S_ROH= 16.1% $STY_{C2+}OH$= 78.5 mg $g_{cat}^{-1}h^{-1}$	[127]
2.5K5Co-In_2O_3	precipitation and impregnation	fixed-bed reactor, T = 380℃, P = 40 bar, H_2/CO_2 = 3	X_{CO2}= 36.6% $STY_{C2+}OH$= 169.6 g $kg_{cat}^{-1}h^{-1}$ $C_{2+}OH/ROH$= 87.4%	[141]
(K_2O)5%/$CuZnFeZrO_2$	co-precipitation and impregnation	fixed bed micro-reactor, T = 250 ℃, P = 30 bar, H_2:CO_2 = 3, GHSV= 3600 h^{-1}	X_{CO2}= 25.49% STY_ROH= 0.32 g/mL·h	[104]

Note: [*1]n/a: not available/given

Table 3

Composition, synthesis technique, experimental conditions and performance of bimetallic and multimetallic-based catalysts as reported in selected works from the literature.

Catalyst	Synthesis method	Experimental conditions	Catalytic activity	Ref.
1%Na-50Co50Fe	oxalate route (using oxalic acid)	fixed-bed reactor, catalyst activation with CO, T = 270̊C, P = 9.2 bar, H_2/CO_2 = 2.5, SV = 2.0 nLgcat^{-1} h^{-1}	X_{CO2}= 22.7% $S_{oxygenates}$= 5.3 mol%	[142]
4 K-X-FeIn/Ce−ZrO_2_T (X = Fe/(Fe+In)= 0.82) (T = 900-calcination temperature)	wetness impregnation and mixing with K_2CO_3	fixed-bed reactor, 0.4 g of the catalyst with 3.0 g of SiC, H_2/CO_2 = 3, P = 100 bar, T = 300̊C, GHSV= 4500 mLg^{-1} h^{-1}	X_{CO2}= 29.6% S_{HAs}= 28.7%	[144]
Pt_1Ru_2/Fe_2O_3	co-precipitation method	batch reactor, T = 200̊C, P = 200 bar, H_2:CO_2 = 8:12, solvent: DMI	activity= 2.4 mmol$_{CO2}$g$^{-}_{cat}$ ^{1}h^{-1} S_{C2+}OH= 36%	[147]
1.23%Pd_2Cu NPs^{*1}/TiO_2	n/a^{*2}	batch reactor, T = 200 ̊C, P = 32 bar, H_2:CO_2 = 3, solvent: H_2O	X_{CO2}= n/a^{*2} S_{Et}OH= 92.0% TOF_{Pd}= 359.0 h^{-1}	[148]
Cu-Co-Zn-Al-T (T = 500 °C reduction temperature)	co-precipitation method	batch reactor, T = 200 ̊C, P = 80 bar, H_2:CO_2 = 3, solvent: THF	STY_{Et}OH= 41 C μmol·g$_{cat}^{-1}$·h^{-1} STY_{Pr}OH= 12 C μmol·g$_{cat}^{-1}$·h^{-1}	[149]

Note: ^{*1}NPs: nanoparticles, ^{*2}n/a: not available/given

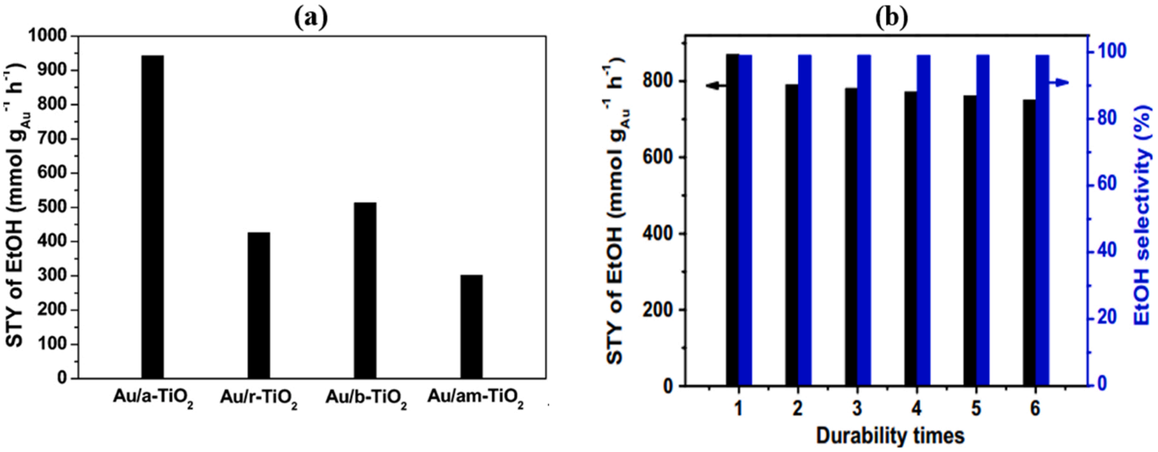

Fig. 3. **(a)** Catalytic activity of Au/TiO_2, using different TiO_2 polymorphs, and **(b)** Recyclability of the best performing catalyst, i.e., Au/a-TiO_2 [93].

(Fig. 3b). Moreover, the authors also investigate the effect that different solvents had on the reaction (an important consideration for batch reactions) and reported that the use of DMF, in comparison with N-methyl-2-pyrrolidone (NMP), cyclohexane, tetrahydrofuran (THF), and water, helped dissolve the CO_2 species and carry them between the TiO_2 surface defects and the Au surface atoms, improving thus, the hydrogenation of CO_2 to EtOH.

Thus, these works [93,94] demonstrated not only that Au can be a very effective CO_2 hydrogenation to higher alcohols catalyst, but also that the use of TiO_2, a supporting material with a high population of oxygen vacancies, is beneficial to the reaction, as it helps tune the metal-support-interaction and activate the CO_2 molecule.

3.1.3. Other noble-based catalysts

We begin the discussion on this sub-section by referring again to the work carried out by Wang et al. [93] (discussed above), because the authors chose to focus on Au/TiO_2 catalysts, after initial tests (carried out in a batch reactor at T = 200 °C, P = 60 bar, CO_2:H_2 = 1:3, using DMF as solvent), showed that STY_{EtOH} followed the order Au/TiO_2 (282.5 mmol g$_{Metal}^{-1}$ h^{-1}) > Rh/TiO_2 (59.6 mmol g$_{Metal}^{-1}$ h^{-1}) > Pd/TiO_2 (50.2 mmol g$_{Metal}^{-1}$ h^{-1}) > Ir/TiO_2 (41.1 mmol g$_{Metal}^{-1}$ h^{-1}) (all noble metals were loaded at 1 wt%). In the same work, they also reported that the STY_{EtOH} for an Au/Co_3O_4 was higher than that of a Pt/Co_3O_4 (128.9 and 60.3 mmol g$_{Metal}^{-1}$ h^{-1}, respectively).

On the other hand, in an earlier work, He et al. [95], again using a batch reactor (T = 200 °C, P = 80 bar, CO_2:H_2 = 1:3), reported that the selectivity to C_{2+}OH followed the order Pt/Co_3O_4 (82.5%) > Rh/Co_3O_4 (65.4%) > Ru/Co_3O_4 (42.4%) > Pd/Co_3O_4 (5.6%) (all noble metals were loaded at 1 wt%). For the Pt-based catalyst, the authors also showed that the effect of loading follows a volcano type trend in relation to S_{C2+OH}, i.e., 0.2Pt (54.4%) < 1Pt (82.5%) > 5Pt (72.5%). The selectivity of the best performing catalyst Pt/Co_3O_4 to C_{2+}OH was also higher in comparison to Pt/ZrO_2 and Pt/CeO_2, which the authors attributed to the formation of oxygen vacancies on Co_3O_4, which, in synergy with Pt, were then able to dissociate H_2O, with H acting as a further source of H_2, at the metal-support interface. The values reported above were achieved when H_2O-DMI (1,3-dimethyl-2-imidazolidinone) was used as solvent, which needs however caution in handling, as it is toxic. That being said, the authors also put a lot of emphasis on investigating the effect of different solvents (H_2O, DMI, NMP (N-methyl-2-pyrrolidone), cyclohexane, n-decane, and mixtures of these with H_2O), and concluded that the best selectivity to HAs was achieved in the presence of polar solvents (S_{HAs} was exceedingly low when non-polar solvents were used), likely because alcohols are also polar compounds. Unfortunately, the authors have not provided values for the conversion of CO_2 for any of the catalysts discussed above, which somewhat hampers the assessment of their potential for HAs production. As a side note, the low selectivity to ethanol reported by Wang et al. [93] regarding the Pt-based catalysts (discussed above), in comparison to He et al. [95], may be explained by the use of DMF as solvent, which although polar, it also is aprotic, meaning that it does not have the capacity to donate protons and thus promote the production of ethanol.

Considering fixed-bed reactors, the only works that we have found in the literature that report on the performance of Pt-based catalysts for the hydrogenation of CO_2 to higher alcohols have been carried out by Li and co-workers [56,96]. However, the first study that this group published [96], although testing Pt/Co_3O_4 catalysts, placed its emphasis on the investigation of the effect that different morphologies of Co_3O_4 (nanorods and nanoplates) have on catalytic performance; one of the main conclusions drawn was that it was the partly reduced Co_3O_4 nanorods that had a significant effect on HAs production. Moreover, in their subsequent work [56] (discussed in detail in the section dealing with Co-based catalysts), they reported that the STY of HAs on Pt/Co_3O_4 (1.5 mmol g_{cat}^{-1} h^{-1}) was lower than that of Co_3O_4 (1.6 mmol g_{cat}^{-1} h^{-1}), at the same reaction conditions.

3.1.4. *Single atom catalysts (SACs)*

Single atom catalysts (SACs) combine the advantages of both homogeneous (atomic dispersion) and heterogeneous catalysts (easy separation), as the active metallic species either exist as isolated single atoms stabilized by the support or by alloying with another metal. This concept was first pioneered by Qiao et al. [97] who were able to synthesize a catalyst that consisted exclusively of only single atoms that were anchored on an oxide support (Pt/FeOx) and to show that it was highly active and stable for both CO oxidation (the Pt_1/FeO_x SAC was three times more active than its nano-Pt counterpart), and preferential oxidation (PROX) of CO in a H_2 reach stream.

The first to investigate the effect that SACs have on the hydrogenation of CO_2 for the production of $C_{2+}OH$ was Llorca and his co-workers [98], who synthesized Pd catalysts supported on Fe_3O_4 that contained either only Pd single atoms (0.1 wt% Pd) or Pd clusters (0.4 wt% Pd) or Pd nanoparticles (3 wt% Pd). Initial tests were performed in a fixed-bed reactor at T = 300–400 °C and $CO_2:H_2$ = 1:4. The authors reported outstanding EtOH selectivity for the single atom Pd catalyst, which was 97.5% at 300 °C, while the STY_{EtOH} was 413 mmol g_{Metal}^{-1} h^{-1}, concluding thus, that there is a direct correlation between the Pd particle size and ethanol yield. What is remarkable about this result is that it was achieved at atmospheric pressure. However, X_{CO2} was very low, as it stood at 0.3% at 300 °C, rising to 3.9% at 400 °C. Another drawback was that the catalysts were particularly prone to deactivation, especially at higher temperatures. The authors also investigated the effect of pressure on the 0.1 Pd catalyst and at 30 bar (T = 250 °C, $CO_2:H_2$ = 1:3) recorded a virtually unchanged S_{EtOH} (98%) and an improved X_{CO2} (1.4%); STY_{EtOH} was improved at 440 mmol g_{Metal}^{-1} h^{-1}.

Lou et al. [99], also compared the performance of different sized Pd catalysts in a fixed-bed reactor (T = 240 °C, P = 30 bar, $CO_2:H_2$ = 1:3), using (a) Pd nanoparticles and (b) Pd dimers; both were supported on CeO_2. The authors reported that Pd dimers were remarkably active, giving a tremendously high ethanol selectivity (99.2%) as well as $STY_{ethanol}$ (45.6 $g_{ethanol}$ g_{Pd}^{-1} h^{-1}), outperforming both the nano-Pd/CeO_2, but also other literature catalysts used under similar reaction conditions (Table 1); X_{CO2} stood at 9.2%. The authors inferred that the improved catalyst activity was due to the Pd dimer structure, which has the ability to both optionally promote the C-C coupling reaction and inhibit the production of C_1 products, leading thus the reaction directly to ethanol. Using density functional theory (DFT) simulations the authors further argued that the two-atom structure of Pd dimers enabled the activation of CO_2 via direct dissociation (activation barrier of 0.70 eV) and bound the as formed CO intermediates. As a result, the desorption of CO was prevented (activation barrier of 2.91 eV) and the coupling of CO and $*CH_3$ intermediates (activation barrier of 1.09 eV) was promoted (Fig. 4).

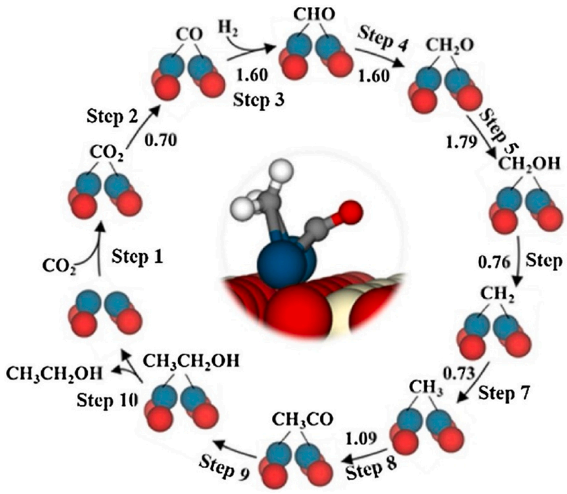

Fig. 4. Schematic representation of the elementary steps and their activation barriers (in eV) for formation of EtOH using the Pd_2/CeO_2 catalyst. The O atoms are represented by the red spheres and the Pd atoms by the blue spheres [99].

Ye et al. [100], took advantage of the opportunities offered by SACs and synthesized a novel catalytic system with Ir atomic active sites that were uniformly distributed on a partially reduced In_2O_3 support; the reduction of In helped to generate oxygen vacancies which then served as anchoring sites for the Ir single atoms. For comparison purposes, the authors also synthesized an Ir/In_2O_3 with a higher Ir loading (1 wt%, when only 0.2 wt% was used to produce the SA catalyst) in which the Ir formed 1–2 nm particles (Fig. 5). Experiments were carried out in a batch reactor (at T = 180–240 °C, P = 60 bar, $H_2:CO_2$ = 5), using H_2O as solvent. The authors were able to obtain outstanding S_{EtOH} (99.7%) and TOF (481 h^{-1}) at the optimum reaction conditions and show that the atomically dispersed Ir and the adjacent Ov on In_2O_3 formed a Lewis acid-base pair that constituted two distinct catalytic centers. In this way, a synergistic effect was created into which the CO_2 dissociation occurred through the adsorption of the C atom to the Ir atoms and the adsorption of one of the O atoms to the In_2O_3 Ov. In agreement with He et al. [95], the authors also argued that the production of ethanol proceeds via a methanol-intermediated mechanism in which the polar solvents, being able to donate protons, aid the production of HAs. Regarding the use of solvents, the authors reported that the S_{EtOH} was in the order of H_2O (99.7%) > DMF (85.6%) > DMI (77.6%). Testing different noble metals as active phases, they also presented the following activity order Ir/In_2O_3 (99.7%) > Rh/In_2O_3 (87.4%) > Pt/In_2O_3 (65.7%) > Pd/In_2O_3 (0.5%).

From the works discussed in this subsection it is clear that the high specific activity achieved using single atom catalysts holds great promise for the production of HAs via the hydrogenation of CO_2, as these systems appear capable of aiding the successful cleavage of the C=O bond and the preferential formation of a C-C bond. Moreover, as by definition, SACs provide highly dispersed metal species, such catalysts can be cost effective alternatives to their nanoparticle and sub-nanometer clusters counterparts. Finally, we note that these works again demonstrate the benefits derived by strengthened metal support interaction, achieved via the use of oxides with abundant oxygen vacancies (Fe_3O_4, CeO_2).

Table 1 provides a summary of the catalytic systems, reactor configurations, reaction conditions and results obtained in terms of CO_2 conversion and ethanol production for the noble-based systems discussed above.

3.2. *Transition metal-based catalysts*

3.2.1. *Cu-based catalysts*

Cu/ZnO-based catalysts have been repeatedly shown to have high activity in methanol reforming, methanol synthesis and the WGSR reaction, with Zn acting as a reservoir for hydrogen atoms, helping to promote the reduction of Cu [101]. To achieve the shift from C_1OH production to $C_{2+}OH$, Cu/ZnO-based catalysts have been combined with Fe, a metal known to be highly active in the RWGS reaction and an alkali component (K or Cs) to regulate the amount of CO and alkyl species produced [102–105].

This idea was first put forward by Takagawa et al. [102], who carried

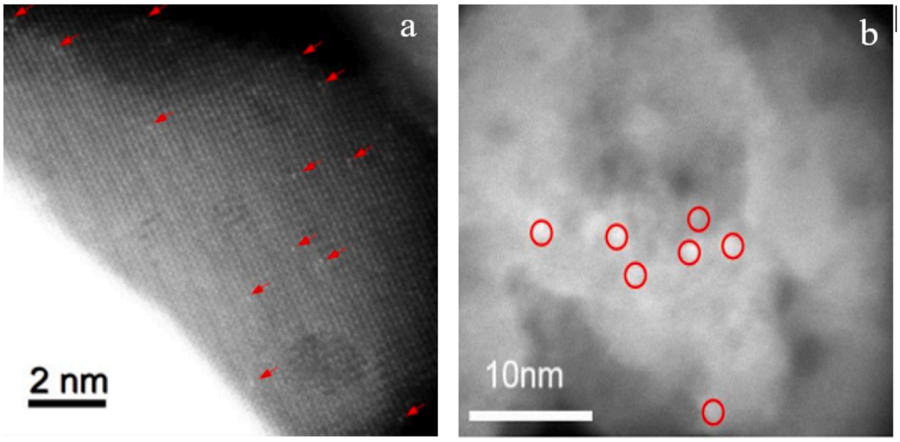

Fig. 5. HAADF-STEM images of the: **(a)** atomically dispersed Ir/In_2O_3, and **(b)** the nanoparticle Ir/In_2O_3 [100].

out one of the earlier studies on the production of HAs via the hydrogenation of CO_2. Experiments were carried out in a fixed-bed reactor at 250 and at 300 ^oC (P = 70 bar, CO_2:H_2 = 1:3). The K/Fe catalyst (K:Fe= 1:5) tested at 250 ^oC showed a low X_{CO2} (3.3%), producing mainly CO (S_{CO}= 73.8%) and C_1-C_5 hydrocarbons (S_{HC}= 20.9%); the selectivity towards ethanol was very low, as it stood at only 1.3%. The increase in the reaction temperature improved X_{CO2} (25.9%), helped decrease the selectivity to CO (S_{CO}= 18.8%) and improved the selectivity to C_1-C_5 hydrocarbons (S_{HC}= 47.9%). Notably, the authors also observed an increase in the selectivity to ethanol (S_{Et}OH= 5.5%) and oxygenates (S_{oxy}= 5.8%, from a meager 0.3%). However, the latter category includes not only propanol and butanol, but also acetaldehyde, methyl acetate and ethyl acetate, and unfortunately, the authors did not quantify the contributions of the individual oxygenates. The CuZn catalyst (Cu:Zn= 1:2) on the other hand, and irrespective of the reaction temperature used, did not produce any EtOH, oxygenates or C_1-C_5 hydrocarbons, but as expected, showed a rather high S_{MeOH} (67% at 250 ^oC and 42.1% at 300 ^oC) and S_{CO} (33% at 250 ^oC and 57.4% at 300 ^oC). The authors then combined the aforementioned elements into a single catalytic system, K/Cu-Zn-Fe (K:Cu:Zn:Fe= 0.08:1:1:3) and went on to successfully produce the desired HAs. Specifically, S_{EtOH} was found at 10.5% at 250 ^oC and 19.5% at 300 ^oC and S_{oxy} at 3.9% at 250 ^oC and 7.4% at 300 ^oC. The increase in the reaction temperature was also beneficial to X_{CO2} (22.3% at 250 ^oC and 44.2% at 300 ^oC). Moreover, as the reaction products exhibited a Flory-Schulz distribution, the authors suggested that the C-C bonds were formed by a mechanism similar to the Fischer–Tropsch reaction. It is noted that the results reported by Takagawa et al. [102] compare favorably with those reported above for Rh-based systems [75–78]. A major disadvantage of the K/Cu-Zn-Fe catalyst was its propensity to deactivation, caused by the segregation of its components, but the authors managed to stabilize the spinel structure of the catalyst by the addition of a fifth element, Cr [102,103]. Time-on-stream results for the K/Cu-Zn-Fe-Cr showed that after a slow drop during the first 40 h of time-on-stream, S_{EtOH} stabilized close to 15% for the rest of the experiment (approximately another 450 h).

Fifteen years later, Chen and co-workers [73], also investigated the hydrogenation of CO_2 to higher alcohols on a K/Cu–Zn catalyst that was promoted with Fe and attempted to clarify the role of Fe on the reaction. The authors carried out the catalytic tests in a fixed-bed reactor, using T = 300 °C, P = 60 bar, and H_2/CO_2 = 3:1. For this purpose, they prepared a series of K/Cu–Zn (K:Cu:Zn= 0.15:1:1) catalysts adding different amounts of Fe (x = 0, 0.25, 0.5, 0.75, 1.0 and 1.5) and reported as optimal the catalyst that contained a medium iron content (x = 0.5 and Fe/(Cu + Zn + Fe)= 0.2 or $CuZnFe_{0.5}K_{0.15}$). For this sample, CO_2 conversion was 42.3%, STY_{ROH} was 0.17 g mL^{-1}·h^{-1} and S_{ROH} was 36.67%. Moreover, the C_{2+}OH/C_1OH ratio was 6.76 (thus, the S_{HAs} was 31.9%). Specifically, the authors reported that an increase in the Fe/(Cu +Zn +Fe) ratio from 0 to 0.2 led to an increase of X_{CO2} (from 25.1% to 45.1%); upon a further increase of this ratio (up to 0.429), X_{CO2} begun to decline (from 45.1% to 33.8%). The same pattern was observed for the selectivity and STY of alcohols which reached the value of 36.67% (from 10.91%) and 0.17 g mL^{-1}·h^{-1} (from 0.04 g mL^{-1}·h^{-1}) at Fe/(Cu +Zn +Fe)= 0.2, before declining to 22.44 wt% and 0.06 g mL^{-1}·h^{-1} (at Fe/(Cu +Zn +Fe)= 0.429), respectively. Thus, the authors were able to show that the selectivity to HAs follows a volcano-shaped relationship to the Cu/Fe ratio. Moreover, based on the findings discussed above, and the physicochemical properties of the materials, the authors were able to conclude that the addition of Fe (at medium concentration) improved the interaction of both Cu-Fe and Zn-Fe, which helped generate dispersed CuO, $CuFe_2O_4$ and $ZnFe_2O_4$ spinel phases. In turn, during the CO_2 hydrogenation reaction, CuO and $CuFe_2O_4$ were reduced to Cu species, while $ZnFe_2O_4$ reduced to FeC_x (low or high Fe concentrations resulted at incomplete reduction). As is well understood, FeC_x promotes CO dissociation, C-C chain growth and the hydrogenation reaction, while Cu promotes the non-dissociation of CO.

Guo et al. [104] also utilized a K_2O (1, 3, 5 and 7 wt%) modified $CuZnFeZrO_2$ catalyst. The tests were carried out in a fixed bed reactor and the authors reported that the highest catalytic performance (STY_ROH= 0.32 g mL^{-1}·h^{-1} and a X_{CO2}= 25.49%) was achieved when K= 5% at T = 250 ℃, P = 30 bar, and H_2/CO_2 = 3:1. In agreement with the works reported above the authors concluded that the addition of K helped improve the catalytic activity and stability.

In another interesting work, Hong and co-workers [105] used Cs (instead of K) and tested x%Cs- $C_xF_yZ_{1.0}$ (CuFeZn) in a fixed-bed reactor, using T = 260–330 °C, P = 50 bar, and H_2/CO_2 = 3:1. The authors initially attempted to clarify the role of Cs during the hydrogenation of CO_2 for HAs synthesis and for this purpose they tested catalysts with different Cs contents (Cs= 0, 1, 2, 3, 5 wt% in $C_{0.9}F_{0.1}Z_{1.0}$). TPR experiments showed that the addition of Cs had a negative effect on catalytic reduction, which in turn affected the hydrogenation ability of the materials, leading to lower CO_2 conversion and methanol selectivity. Moreover, as the authors observed that the increase in Cs content led to an improvement in the CO-free S_{olefin} and S_{HAS}, and to a decline in CO-free $S_{alkanes}$, they surmised that Cs favors alkyl dehydrogenation and CO insertion and inhibits alkyl hydrogenation. These conclusions, in regard to the role of Cs, are in agreement with other literature works reporting on the role of K or other alkali metals [72,106,107]. The best performing catalyst was the one containing 3 wt% Cs, at 310 ^oC, with X_{CO2} ≈ 24% and STY_{C2+OH} ≈ 37 mg g_{cat}^{-1} h^{-1}. The authors also tried to optimize the Cu/Fe molar ratio, and in agreement with Chen and co-workers [73], reported that the relationship to S_{HAs} is volcano shaped. Moreover, and again in agreement with Chen and co-workers [73], they argued that as the Cu/Fe ratio increases, so does the production of non-dissociative CO, while that of CH_4 (dissociative CO) declines, up to an optimal ratio. In other words, the highest performance (the top of the volcano) is achieved when there is a balance between the active sites that are responsible for the dissociation (FeC_x) and non-dissociation (Cu) of CO, which allows the desired amount of CO and alkyl species to be produced. The best performing catalyst was 3%Cs-$C_{0.8}F_{1.0}Z_{1.0}$, at 330 ^oC, with an improved STY_{C2+OH} close to 73 mg g_{cat}^{-1} h^{-1}, a value which is one of the highest reported in the literature for this reaction (Tables 1–3).

Hong and co-workers [108] carried out an additional work on the hydrogenation of CO_2 to HAs, this time using a K modified CuMgZnFe ($C_{1.0}M_{1.5}Z_{0.5}F_{1.0}$) catalyst. The aim of the work was to clarify the role of K, so the K content was varied at 0.1%, 1.4%, 4.6% and 17.6%. Notice that the molar ratio of CZF is different to the work reported above (their previous work). Experiments were carried out in fixed-bed reactor, using T = 320 °C, P = 50 bar, and H_2/CO_2 = 3:1. As expected, the authors showed that the increase in the K content lowered the conversion of CO_2 and favored the production of HAs up to a K content of 4.6 wt%, i.e., the relationship between HAs synthesis and K content is volcano-shaped (Fig. 6). Further, using in-situ DRIFTS and chemisorption studies the authors were able to confirm that the synthesis of HAs follows a CO-mediated insertion pathway. The role of K is similar to that discussed for Cs above, i.e., it helps regulate the hydrogenation capacity, lowers the production of methanol and balances the active sites that are responsible for the dissociation and non-dissociation of CO, which allows the desired amount of CO and alkyl species to be produced.

In summary, as Cu/ZnO-based catalysts are highly active in methanol synthesis, the effort to shift their activity from C_1OH production to $C_{2+}OH$ has focused on the addition of an alkali metal (K or Cs) in combination with Fe, a transition metal known for its high activity in the RWGS reaction. The aim is to regulate the amount of CO and alkyl species produced, by striking a balance between FeCx species, which promote the dissociation of CO, the C-C chain growth and the hydrogenation reaction, and of the Cu species, which promote the non-dissociation of CO. Alkali metals help lower the production of alkanes via the hydrogenation of the intermediates (C_xH_y), which improves HAs synthesis, lower the production of methanol and balance the active sites that are responsible for the dissociation and non-dissociation of CO.

3.2.2. Mo-based catalysts

Mo based catalysts, such as MoS_2, Mo_2C, MoO_x, and MoP, modified with alkali and/or transition metals have been applied effectively over the past four decades for the hydrogenation of CO to alcohols such as methanol, ethanol and propanol [109–112]. In addition, $CoMoS_2$ catalysts, modified with alkali metals, have been shown to work for Fischer–Tropsch synthesis and for the RWGS reaction [113–116]. Thus, this dual functional property has made them a candidate for HAs production via CO_2 hydrogenation.

Nieskens et al. [117] was one of the first groups that tested a K modified CoMoS catalyst in higher alcohols synthesis via CO_2 hydrogenation. The experiments were conducted in a fixed-bed reactor under varied H_2:CO_2 ratios (1 and 3) as well as temperatures (310 and 340 °C) while the pressure was set at 104 bar. From the experimental results presented, HAs formation was rather low, as these catalysts were more selective towards methanol and CO production. However, the authors also showed that an increase in the reaction temperature (from 310 to 340 ^oC), while using H_2:CO_2 = 3:1, was beneficial to HAs production as S_{EtOH} increased from 4.2% to 5.5% and S_{PrOH} from 0.2% to 0.5%, while S_{MeOH} dropped from 31.0% to 20.0%; S_{CO} remained virtually unchanged (at around 58%). Surprisingly, the authors reported that the decrease in the H_2:CO_2 from 3:1–1:1, affected only the selectivity to methanol (leading to lower values), irrespective of the temperature at which the reaction was carried out. Regarding S_{HAs}, while still examining the effect of the lower H_2:CO_2 ratio, at 310 ^oC, the values given for both ethanol and propanol were identical (S_{Et}OH= 4.2%, S_{Pr}OH= 0.2%), while at 340 °C, there was a slight drop for ethanol (from 5.5% to 4.6%) and a small increase for propanol (from 0.5% to 0.7%). As expected, CO_2 conversion was higher at the higher H_2:CO_2 ratio, and increased somewhat with the increase in the reaction temperature (28–32%).

A similar catalytic system was studied by Liu et al. [37] who investigated the influence of different K/Mo (0–1.2) and Co/Mo (0–1.2) molar ratios, under different reaction conditions (T = 280–340 °C, P = 30–120 bar, H_2:CO_2 = 3:1), in the performance of a series of $Mo_1Co_xK_y$ sulfide catalysts, in a fixed-bed reactor. From the experimental results, the best catalytic performance was achieved by the $Mo_1Co_1K_{0.8}$ system, at 320 °C and 120 bar, with a total CO_2 conversion around 22%, while the selectivity to total alcohols and C_{2+} alcohols reached the values of 82% and 11%, respectively, at the end of a time-on-stream experiment. To improve the catalytic performance the authors also examined the effect of different additives (SiO_2, Al_2O_3, TiO_2, activated carbon). Although they had identified the $Mo_1Co_1K_{0.8}$ as the best performing system, these experiments were carried out using a $Mo_1Co_1K_{0.6}$ catalyst, probably because they had previously argued that over a K/Mo ratio of 0.3 there was not much difference in performance. The experimental results (Fig. 7) revealed that the CO_2 conversion was rather similar between SiO_2-, Al_2O_3-, and TiO_2-containing catalysts (~24.5%) in comparison to the unmodified $Mo_1Co_1K_{0.6}$ catalyst (25.5%). Similarly, the SiO_2-, Al_2O_3- and TiO_2 additives favored the RWGS reaction giving CO selectivity values of 82.5%, 80.5% and 79.9%, respectively, higher than that for the unmodified $Mo_1Co_1K_{0.6}$ catalyst (73.2%). However, the addition of activated carbon (AC), although led to an important decrease of CO_2 conversion from 25.5% to 8.5%, it also resulted at a catalyst that was more selective towards C_{2+} alcohols (15.5%) –in contrast with the other modifiers (3.4–6.3%) and the unpromoted $Mo_1Co_1K_{0.6}$ catalyst (5.8%)– and less selective towards methanol (49.7% vs ~85%). The authors attributed the higher HAs production to an improvement in the Mo-Co particles interaction, and to the adsorption strength of CO_2 and H_2 molecules on the surface of the activated carbon.

The same group published a subsequent work [118] in which they compared the performance of the aforementioned $Mo_1Co_1K_{0.6}$-AC *bulk-phase* catalyst, with Mo_1-Co_x-K_y sulfide catalysts that were *supported* on activated carbon using a fixed-bed reactor (T = 320 °C, P = 50 bar,

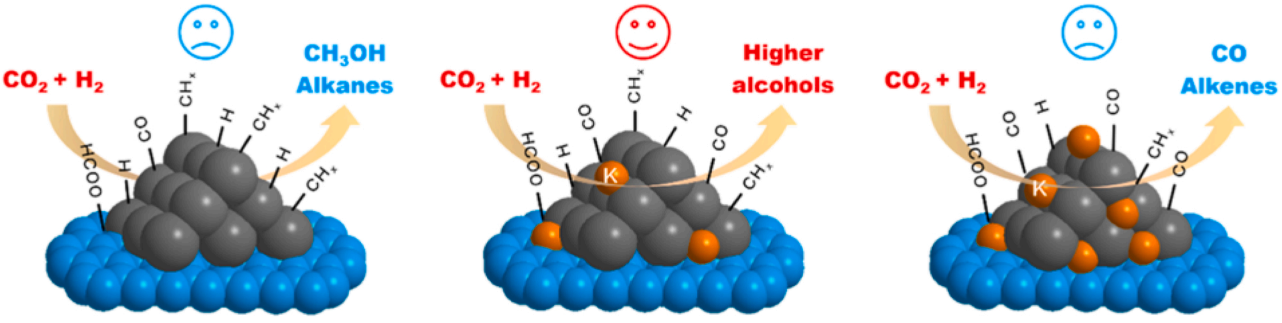

Fig. 6. Schematic representation of the product distribution in relation to the K content [108].

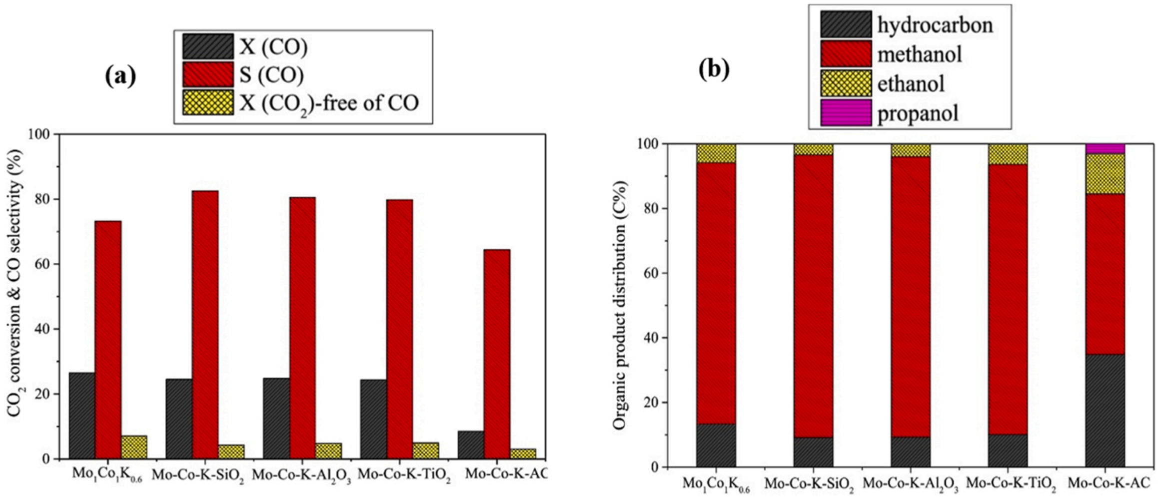

Fig. 7. Performance of the $Mo_1Co_1K_{0.6}$ catalyst with different additives: **(a)** X_{CO}, S_{CO} and X_{CO2}, and **(b)** S_{HC}, S_{MeOH}, S_{EtOH} and S_{PrOH} (reaction conditions: T = 320 °C, P = 50 bar, H_2:CO_2 = 3, GHSV= 3000 mL g^{-1} h^{-1}) [37].

H_2:CO_2 = 3). Unfortunately, it is not possible to provide a direct comparison between these works, i.e., [37] and [118], as the authors used somewhat different reaction conditions (apart from a smaller diameter reactor, the GHSV used in the latter study was calculated based on catalyst volume instead of catalyst mass, as in the previous work). The authors first showed that the addition of excess amounts of activated carbon to the *bulk* catalyst (Mo:AC= 9, while in the previous work Mo:AC= 185) resulted at a dramatic drop in S_{MeOH}, and S_{EtOH} (S_{CO2} and S_{CO} remained unaffected, and S_{HC} increased by a factor of 2), probably because of a reduction in the amount of the active phase available to the reactants. However, when comparing the performance of the *bulk* catalyst containing the excess amount of AC ($Mo_1Co_1K_{0.6}$-AC-9%) to that of a *supported* catalyst containing also the same amount of activated carbon ($Mo_1Co_1K_{0.6}$/AC-9%), they concluded that the *supported* catalyst had a higher X_{CO2} (23.4% compared to 8.1%) and S_{EtOH} (5.8% compared to 1.2%). For the supported catalysts, the authors, using this time a $Mo_1Co_{0.3}K_{0.9}$/AC catalyst, also showed that using even higher amounts of activated carbon (Mo:AC= 3 instead of Mo:AC= 9) ratio were detrimental to both X_{CO2} and S_{EtOH}. However, it is also noted that the $Mo_1Co_1K_{0.6}$/AC (which was the best performing catalyst that was *supported* on AC), had a rather similar performance to the catalyst containing no activated carbon ($Mo_1Co_1K_{0.6}$). Unfortunately, the authors never tested a $Mo_1Co_1K_{0.6}$/AC catalyst with a Mo:AC= 185, which would have provided a more concrete answer over the improvement that the *supported* AC-based catalyst would have brought.

Summarizing, although Mo-based catalysts, modified with alkali and/or transition metals, have been successfully applied for the hydrogenation of CO to alcohols and $CoMoS_2$ catalysts, modified with alkali metals, have been shown to work for Fischer–Tropsch synthesis and the RWGS reaction, their performance for HAs production is not encouraging, as from the works reported in the literature, the shift from methanol and CO production to C_{2+} alcohols has not materialized to a satisfactory extend.

3.2.3. Co-based catalysts

Cobalt based catalysts have been widely used for the production of heavy hydrocarbons through Fischer–Tropsch synthesis, but they have very low WGS activity and act primarily as methanation catalysts when CO_2 is used instead of CO [119,120]. Gnanamani et al. [121] however, utilized a Co (20 wt%) supported on SiO_2 catalyst that was promoted with Na (1 wt%) and attempted to lower its methanation activity by controlling the chemical nature of the cobalt phases through the activation procedure (the authors used H_2, syngas and CO). Tests were carried out in a fixed-bed reactor (T = 220 °C, P = 19 bar and H_2:CO_2 = 3) and the authors observed that the X_{CO2} conversion dependent on the reducing gas, in the order of CO > syngas > H_2 (Fig. 8). Moreover, CH_4 selectivity followed the opposite trend, i.e., the highest S_{CH4} was recorded when pretreatment was undertaken using H_2, and the lowest when it was carried out under CO. In addition, the highest alcohol selectivity was recorded when reduction was carried out under CO atmosphere. These findings helped the authors conclude that the carburization of the Na-Co/SiO_2, which occurred under CO, helped lower the hydrogenation to methane activity of the catalyst, either through Na deposition on Co_2C or by stabilization of the Co_2C on to the catalytic surface.

Another interesting study using Co-based catalysts was carried out by Li and co-workers [99]. Specifically, based on their previous work regarding Pt/Co_3O_4, where they concluded that partly reduced Co_3O_4 nanorods had a significant effect on HAs production, they subsequently compared the performance of mesoporous Co_3O_4 (Co_3O_4-m), which they synthesized using a high surface (728.2 m^2 g^{-1}) mesoporous silica (KIT-6) as a hard template, with that of Co_3O_4 nanoparticles (Co_3O_4-np), and of Pt supported on the Co_3O_4-m [56]. The catalytic tests were carried out in a fixed-bed reactor using relatively mild reaction conditions (T = 160 or 200 °C, P = 20 bar, H_2:CO_2 = 3). Initially, the authors evaluated the activity of the Co_3O_4-m and Co_3O_4-np at different reduction (250 and 300 °C) and reaction temperatures (160 and 200 °C). As expected, given that CO_2 conversion depends upon the availability of

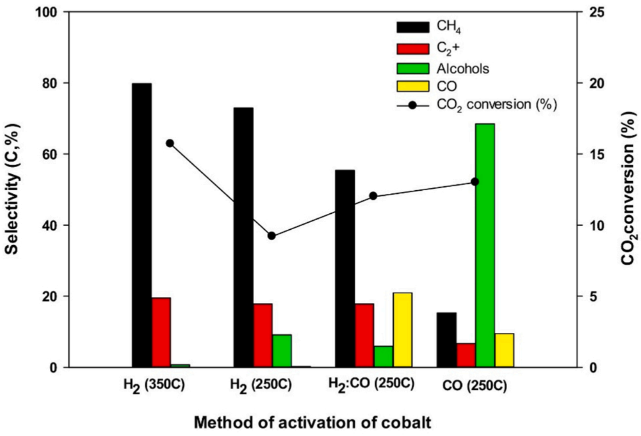

Fig. 8. Effect of activation procedure on the product selectivity during CO_2 hydrogenation using a Na-Co/SiO_2 catalyst (reaction conditions: T = 220 °C, P = 19 bar, H_2:CO_2 = 3:1) [121].

Co^0, higher reduction temperatures led to higher X_{CO2} values, for both catalysts. Moreover, higher reaction temperatures were beneficial to the production of HAs, as the STY rose from 1.3 to 1.6 mmol g_{cat}^{-1} h^{-1} for the Co_3O_4-m and from approximately 0.1 to 0.25 mmol g_{cat}^{-1} h^{-1} for the Co_3O_4-np (Fig. 9). As the distribution of CoO, *fcc*-Co (fcc: face centered-cubic) and *hcp*-Co (hcp: hexagonal close-packed) was similar for both catalytic systems (albeit at different reduction temperatures), the authors concluded that the improvement in the production of HAs was owned to the mesoporous structure of the Co_3O_4-m catalyst. The authors attempted to explain this by arguing that the mesopore channels helped the formation of C-C bonds, as they confine the $*CH_x$ species, forcing them to come into contact with one another, forming long chain carbon species, preventing thus their undesired hydrogenation to CH_4. The authors also tried to further improve the performance of the Co_3O_4-m, by synthesizing a Pt/Co_3O_4-m however, although S_{CH4} declined and S_{ROH} increased, the STY of HAs was slightly lower than the non-noble metal Co_3O_4-m.

The group of Xiao [122,123] also investigated the performance of Co-based catalysts during the hydrogenation of CO_2. In the first of these works [122], the authors prepared cobalt catalysts derived from a Co-alumina layered double hydroxide (LDH); denoted as $CoAlO_x$-T, with T indicating different reduction temperatures (from 300 to 650 ^oC). Catalytic tests were carried out in a batch reactor (T = 140 or 200 °C, P = 40 bar, H_2:CO_2 = 3) using H_2O as solvent. Among the tested catalysts, the best performance was recorded for the $CoAlO_x$ that was reduced at 600 ^oC, giving an ethanol selectivity of 92.1% and an alcohol STY of 0.444 mmol g^{-1} h^{-1} at 140 ^oC (Fig. 10). Comparative tests showed that this performance was higher than a commercial Co_3O_4, a Cu/ZnO/Al_2O_3 and alumina-supported Fe and Ni catalysts. The authors attributed this performance to the ability of the $CoAlO_x$-600 to promote the formation of acetate from formate species, by insertion of $*CH_x$, which consequently leads to ethanol production. Nonetheless, it is noted that the STY_{EtOH} value of 0.444 mmol g^{-1} h^{-1} is approximately 4.5 times lower than that reported by Wang et al. [93] for an Au NC-TiO_2 discussed above (albeit the STY reported by Wang et al. [93] was achieved at 200 ^oC and at P = 60 bar).

In the second work from the group of Xiao [123], the authors employed again the $CoAlO_x$ catalysts discussed in the previous paragraph and used Ni, Pd and Pt as an additive ($Co_mM_nAlO_x$) in an effort to affect the production of $*CH_x$ and *HCOO intermediaries towards C_{2+} production. It is noted that catalysts with different Co/Ni ratios were also synthesized. Catalytic tests were again carried out in a batch reactor (T = 140 or 200 °C, P = 40 bar, H_2:CO_2 = 3) using H_2O as solvent and from the results obtained it was obvious that the addition of the promotes helped enhance ethanol production in comparison with the bare $CoAlO_x$. Specifically, STY_{EtOH} was 11.2 mmol g_{cat}^{-1} for the $Co_mPt_{0.05}AlO_x$ and 10.4 mmol g_{cat}^{-1} for the $Co_mPd_{0.05}AlO_x$. However, the highest STY_{EtOH} (15.8 mmol g_{cat}^{-1}) was achieved using the $Co_{0.52}Ni_{0.48}AlO_x$, which they attributed to the formation of a CoNi alloy that had a profound effect of the adsorption of CO_2 and in turn, to the hydrogenation of *HCOO species.

From the works discussed in this sub-section it becomes clear that the performance of Co-based catalysts depends to a large extent on the formation of Co^0, CoO, $Co^{\delta+}$ and Co_2C and the synergy between these species. These Co hetero sites depend on the reduction process, the presence of alkali metals and the interaction between Co and the supports/promoters. However, these works also make clear that these systems exhibit low CO_2 conversion and HAs selectivity, in comparison with other systems reported in the literature, with obvious drawbacks regarding commercialization. More information, specifically on Co-based catalysts, for the CO_2 to higher alcohols hydrogenation, can be found in a recent review paper by Liu et al. [35].

3.2.4. *Fe-based catalysts*

Iron has been widely used for the conversion of CO_2 [124] and for the formation of hydrocarbons via Fischer–Tropsch synthesis. It has also been shown to have high activity in the RWGS reaction, and to have the ability to dissociatively adsorb the produced CO [125,126]. CO dissociation in particular, occurs through the formation of a σ-bond between iron and carbon, and the simultaneous donation of Fe electrons to the $2\pi^*$ orbital of carbon monoxide. This causes a strengthening of the Fe-C bond, while it also weakens the C-O bond to a point where CO dissociation is possible. Thus, as discussed above, Fe has been utilized as supporting material in Pd-based catalysts [98], as a promoter in Rh-based systems [75–78] or in combination with other transition metals (Cu-Zn [73,102,103]).

Yao et al. [127] however were able to show that a monometallic Fe-based catalyst, promoted only with Na and S (FeNaS) was capable of producing HAs during the hydrogenation of CO_2. Specifically, FeNaS-x catalysts with different sulfur content (x = 0.03, 0.1, 0.6, 3.0) were evaluated using a fixed-bed reactor (T = 320 °C, P = 30 bar, H_2:CO_2 = 3), and the FeNaS-0.6 was found to exhibit the optimal CO_2 conversion (32.0%) as well as alcohols selectivity (16.1%) and C_2OH space-time yield (78.5 mg $g_{cat}^{-1}h^{-1}$). They argued that this notable performance, for a non-noble, monometallic catalyst, was due to the excellent synergistic interaction between Na and S in the Fe-based catalyst, with Na assisting the dissociation of CO, and S, helping to provide additional Fe sites where the non-dissociation of CO was possible. Thus, this work showed that Fe can favor the growth of the carbon chain required for HAs production in single component systems.

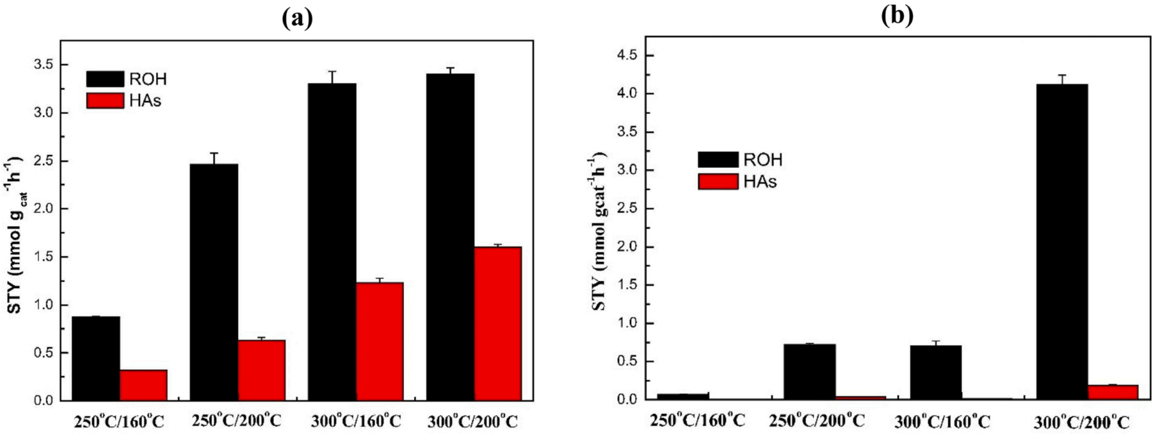

Fig. 9. Space time yield of total and higher alcohols using the: **(a)** Co_3O_4-m, and **(b)** Co_3O_4-np (Reaction conditions: T = 160 or 200 °C, P = 20 bar, H_2:CO_2 = 3, GHSV= 6000 mL g_{cat}^{-1} h^{-1}) [56].

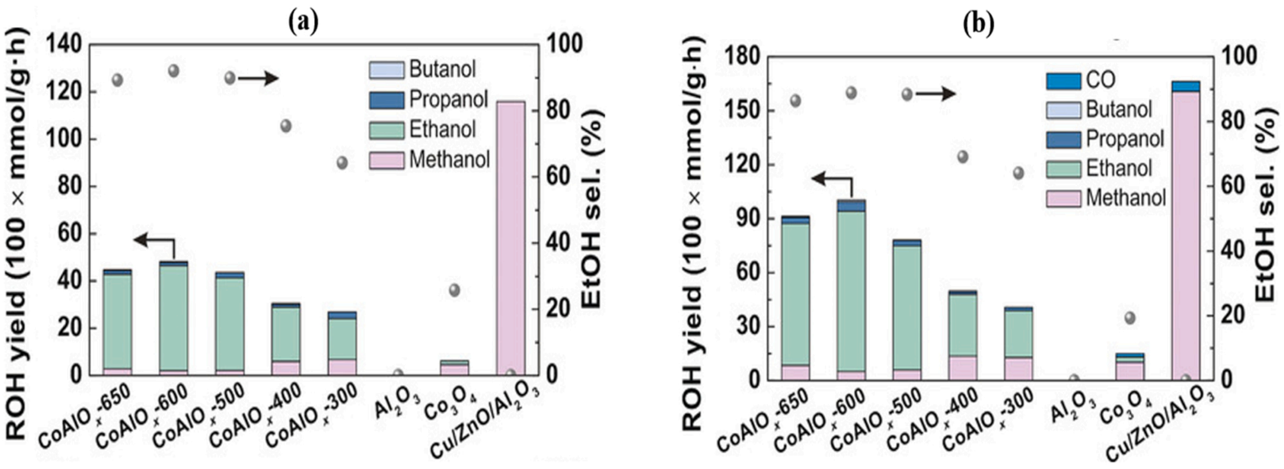

Fig. 10. Comparison of the activity obtained over different $CoAlO_x$-T (T indicates reduction temperatures from 300 to 650 °C) at P = 40 bar, H_2:CO_2 = 3: (a) T = 140 °C, and (b) T = 200 °C [122].

3.3. Post-transition metal-based catalysts

Indium, which derives its name from the indigo color line of its spectrum, was one of the least explored elements in heterogeneous catalysis, despite published works that demonstrate that In-based systems show high activity and selectivity in catalytic reactions that involve the transformation of CO_2, such as its photocatalytic reduction to CO and its electrochemical conversion to formic acid [128–130]. However, after the seminal works of Ge and his co-workers [131,132], who, using DFT studies, showed that In_2O_3 is highly active in the adsorption and activation of CO_2, In_2O_3-based catalysts emerged as one of the most promising materials for the hydrogenation of CO_2 into methanol [133–139] and gasoline range hydrocarbons [140].

Following on these footsteps, Limtrakul and his co-workers [141] became the first group that studied the performance of unpromoted In_2O_3 catalysts and In_2O_3 catalysts that were promoted with K or/and Co, in the hydrogenation of CO_2 to HAs. The authors carried out the experimental work on a fixed-bed reactor (T = 260–380 °C, P = 40 bar, H_2:CO_2 = 3). The initial screening of the materials was carried out at 380 °C and the results showed that the unpromoted In_2O_3 catalyst was not able to produce higher alcohols, but had the capacity to transform CO_2 to CO, without it being further dissociated to C and O. Moreover, despite the fact that the In_2O_3 catalyst promoted with only K or only Co, were also not selective towards HAs, the authors were able to deduce that K-In_2O_3 was capable to retard the formation of CH_4 and promote the production of methanol, while Co-In_2O_3 led to an increase in the production of methane, and also produced a small amount of ethanol. Thus, the authors synthesized In_2O_3 catalyst that utilized both K and Co as promoters and showed that the 2.5K5Co-In_2O_3 catalyst not only achieved a significantly high $C_{2+}OH$ distribution of 87.4% in the total alcohol products, but also exhibited one of the highest HAs STY reported in the literature (169.6 g kg_{cat}^{-1} h^{-1}); notably, the catalyst was stable for > 200 h. A combination of XPS and XANES analysis helped the authors to conclude that the improved catalytic performance achieved using both promoters was due to the formation of K-O-Co sites which strengthened the interaction of H_2 with the catalytic surface. This in turn, suppressed the hydrogenation of C_xH_y species to hydrocarbons and allowed the insertion of carbon monoxide into the C_xH_y * intermediate species, leading to the formation of higher alcohols (Fig. 11).

Table 2 below presents information on the catalyst formulation, reactor configuration, reaction conditions and performance in terms of CO_2 conversion and ethanol production for transition and post-transition metal systems discussed herein.

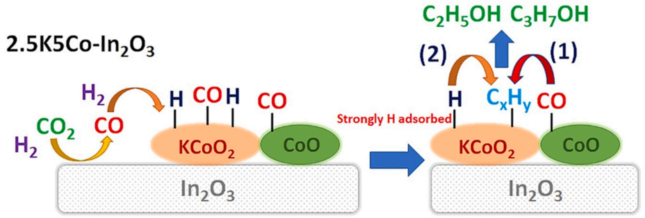

Fig. 11. Proposed mechanism for the formation of HAs over the 2.5K5Co-In_2O_3 catalyst [141].

3.4. Bimetallic catalysts and multimetallic/multifunctional catalysts

As mentioned above, cobalt based catalysts are widely used for the production of heavy hydrocarbons through Fischer–Tropsch synthesis, but they have very low WGS activity and act primarily as methanation catalysts when CO_2 is used instead of CO [119,120]. However, Gnanamani et al. [121], discussed above, showed that for a Co/SiO_2 catalyst, its promotion with Na and its activation with CO, helped create carburized Co, with the system (Na-Co/SiO_2) then being selective towards alcohols. The authors sought to exploit this finding in a subsequent work [142] in which they attempted to keep Fe and Co in proximity in a carburized form. To do so, the authors synthesized a series of Co-Fe bimetallic oxalates, i.e., $Co_{0.9}Fe_{0.1}$, $Co_{0.5}Fe_{0.5}$, $Co_{0.25}Fe_{0.75}$, as well as monometallic Fe and monometallic Co and tested them in a fixed-bed reactor at moderate temperature and pressure (T = 200–270 °C, P = 9.2 bar, and H_2:CO_2 =2.5). Initially, they were able to show that the addition of Fe, up to 50% ($Co_{0.5}Fe_{0.5}$), had a positive effect on catalytic performance, as by increasing the Fe content, the selectivity to C_2-C_4 hydrocarbons and oxygenates also increased, while S_{CH4} decreased; the conversion of CO_2 also decreased. It is noted that pre-treatment (activation) for all the above-mentioned catalysts was carried out using CO. Subsequently, using the $Co_{0.5}Fe_{0.5}$ catalyst, the authors sought to clarify (similarly to their previous work, i.e., ref. [121]) the effect that metallic or carburized forms of Co-Fe have on catalytic performance under different pre-treatment conditions, using either H_2 or syngas or CO. They again showed that the use of CO was beneficial, as it resulted at a material that was less selective towards CH_4. Finally, the authors investigated the effect of alkali metal addition, by promoting the $Co_{0.5}Fe_{0.5}$ either with 1 wt% Na or 1.7 wt% K, and concluded that catalytic performance further improved upon alkali promotion, as the 1Na-$Co_{0.5}Fe_{0.5}$ and 1.7 K-$Co_{0.5}Fe_{0.5}$ showed a higher selectivity to oxygenates and a decrease in the selectivity of CH_4. Gnanamani et al. [143] produced yet another work on the CO_2 hydrogenation to higher alcohols, again utilizing a Co-Fe system that was promoted with K. The authors, despite concluding in ref. [142] that very high Fe contents (over 50%) do not bring an improvement upon catalytic performance, in this study, they synthesized a $Fe_{0.9}Co_{0.1}$ catalyst and investigated the effect of the addition of different K contents (0, 0.5, 1.0, 2.0, 3.0 wt%) at low reaction temperature and pressure ($T = 240\ ^{o}C$, $P = 12$ bar, $H_2:CO_2 = 3$), using a fixed-bed reactor. Again, the carburized form of cobalt was formed using an oxalate precursor and under pretreatment with CO, while the use of K as promoter helped produce FeC and graphitic carbon on the surface of Fe during the activation procedure. The authors concluded that the addition of small quantities of K (up to 1 wt%) lowers the selectivity to HC and improves the selectivity to CO and oxygenates. However, they observed that increased amounts of K (over 1 wt%) lower the selectivity to ethanol and promote the formation of acetic acid.

As mentioned above, a number of researchers have tried to utilize the properties of transition metals used in the synthesis of methanol (Cu-Zn) with those of metals known to work on Fischer–Tropsch synthesis (Fe, promoted with an alkali metal), by combining them into single catalytic systems [72,73,102,103]. Xi et al. [144], working under the same principle, replaced the CuZn part of the catalyst with In_2O_3 (as mentioned above, this post-transition element has recently emerged as one of the most promising materials for the hydrogenation of CO_2 into methanol [133–139]). Moreover, as a number of works have shown that oxygen vacancies are the active sites for CO_2 activation [81,93–95], the authors chose to utilize Ce-ZrO_2 as supporting material (with a Ce:Zr ratio of approximately 1:5), as it is well known for its ability to act as an oxygen buffer, storing/releasing oxygen via the Ce^{3+}/Ce^{4+} redox couple [145,146]. Thus, the authors synthesized a series of FeIn/Ce-ZrO_2 catalysts that were promoted with K and carried out the catalyst testing in a fixed-bed reactor at $T = 300\ ^{o}C$, $P = 100$ bar, and $H_2:CO_2 = 3$. Initially, they examined the effect of the addition of K, utilizing a Fe:In ratio of almost 1:1 (K-0.48FeIn/Ce-ZrO_2) and carrying out the catalyst activation procedure with CO as the reducing agent. The authors were able to show that the addition of a small amount of K (1%) helped improve X_{CO2} (from 15.1% to 18.9%) and led to a decrease in the selectivity to methanol and to an improvement in the selectivity to HAs. A further increase of the K content to 4% brought about a small improvement in the S_{HAS} (and a subsequent drop in S_{MeOH}), but it also resulted at a slight decrease in the X_{CO2}. Moreover, a further increase in the K content did not result at a further improvement in the selectivity to HAs; rather it was the selectivity to CO that continued to increase (Fig. 12a). Using the 4 K-0.48FeIn/Ce-ZrO_2 the authors also investigated the effect that different reducing agents (N_2, H_2, CO) have on catalytic performance, and showed that activation with CO lead to the highest S_{HAS}, probably because it helped the formation of FeC species. These in turn acted as active centers, helping to promote the RWGS reaction, the dissociation of CO and the C-C coupling reaction. The authors next turned their attention to the investigation of the Fe/In ratio, by first showing that only the presence of Fe could lead to the production of HAs. Specifically, the catalyst that did not contain Fe (4 K-In/Ce-ZrO_2) was selective towards methanol and CO, while the catalyst that contained only Fe (4 K-Fe/Ce-ZrO_2,) was selective towards hydrocarbons and HAs (Fig. 12b), in agreement with the earlier work reported by Takagawa et al. [102]. After testing various Fe/(Fe+In) molar ratios, they showed that the best performance towards HAs was achieved by the 4 K-0.82FeIn/Ce-ZrO_2, although the improvement in relation to the Fe-only containing catalyst was rather small.

He et al. [147] prepared and tested, for the CO_2 to C_{2+} alcohols reaction, Pt-Ru supported on Fe_2O_3 catalysts, with different Pt/Ru molar ratios (1:2, 1:1, 1:3). The experimental work was carried out in a batch reactor, between 160 and 200 °C and at 200 bar, using the 1,3-dimethyl-2-imidazolidinone (DMI) as solvent. The results indicated that the optimal composition was the Pt_1Ru_2/Fe_2O_3 catalyst, which showed higher activity (2.4 $mmol_{CO2}g^{-1}_{cat}h^{-1}$) and $C_{2+}OH$ selectivity (36%) than the monometallic Fe_2O_3-supported catalysts (Pt/Fe_2O_3 or Ru/Fe_2O_3); importantly, the catalyst was stable and active for five cycles. The authors also showed that an increase in CO_2 and/or H_2 pressure led to an increase in CO_2 conversion and $C_{2+}OH$ selectivity, due to the enhanced solubility of reactants. This improved catalytic performance was attributed to a synergistic effect between Pt and Ru.

Bai et al. [148] synthesized ordered Pd-Cu nanoparticles (NPs) supported on different oxides (SiO_2, CeO_2, Al_2O_3 and TiO_2) and investigated the optimal conditions (Pd/Cu ratio, support, reaction temperature) for the selective CO_2 hydrogenation to ethanol. The authors utilized a batch reactor, and experiments were carried out at 150, 175 and 200 °C, at 32 bar and $H_2:CO_2 = 3$, using H_2O as solvent. Among the different catalytic systems, Pd_2Cu/TiO_2 exhibited the highest catalytic performance and stability (6 cycles). Moreover, an increase in reaction temperature from 150 to 200°C led to a significant increase in the C_2H_5OH yield (from 10 $mmolg^{-1}h^{-1}$ to 40 $mmolg^{-1}h^{-1}$) and selectivity (from 78.1% to 92.0%); the TOF_{Pd} was recorded at 359.0 h^{-1}. This excellent result was attributed to the existence of oxygen vacancies on the TiO_2 surface and the charge transfer, which enhanced the CO_2 hydrogenation via prompting the hydrogenation of *CO to *HCO species.

In another recent study, Li et al. [149] prepared a series of Cu-Co-Zn-Al catalysts, under different reduction temperature (300, 400,

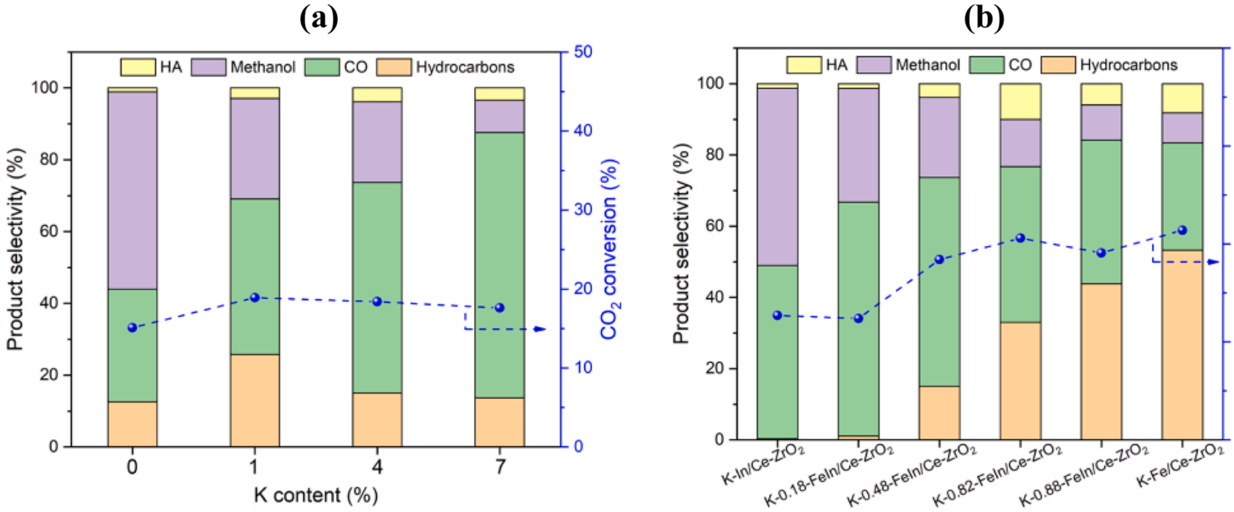

Fig. 12. X_{CO2} and product selectivity for the: **(a)** K-0.48FeIn/Ce-ZrO_2 catalysts (different K contents), and **(b)** 4 K-In/Ce-ZrO_2, K-Fe/Ce-ZrO_2, K-FeIn/Ce-ZrO_2 (different Fe/(Fe+In) molar ratios) (reaction conditions: $T = 300\ ^{o}C$, $P = 100$ bar, and $H_2:CO_2 = 3$, GHSV= 4500 mL g^{-1} h^{-1}) [144].

500, 600 and 700 °C), to catalyze the direct CO_2 hydrogenation to alcohols (methanol, ethanol, n-propyl alcohol). Experiments were carried out in a batch reactor under $T = 200$ °C, $P = 80$ bar and H_2:$CO_2 = 3$, using tetrahydrofuran as solvent. From the studied catalysts, the Cu-Co-Zn-Al-500 exhibited the best performance with carbon yields of 116 $C_{\mu mol} \cdot g_{cat}^{-1} \cdot h^{-1}$ (total carbon), 31 $C_{\mu mol} \cdot g_{cat}^{-1} \cdot h^{-1}$ (methanol), 41 $C_{\mu mol} \cdot g_{cat}^{-1} \cdot h^{-1}$ (ethanol), 12 $C_{\mu mol} \cdot g_{cat}^{-1} \cdot h^{-1}$ (n-propanol), and 32 $C_{\mu mol} \cdot g_{cat}^{-1} \cdot h^{-1}$ (isopropyl ether) arguing that the sheet-like morphology of the catalyst led to higher catalytic performance due to the plethora of active sites on its surface. Surprisingly, the catalysts activated at high temperatures (Cu-Co-Zn-Al-600, Cu-Co-Zn-Al-700) favored the production of C_3 alcohols (propanol) and their derivatives (di-isopropyl ether) while the Cu-Zn-Al catalyst led to the production of C_1 products. Further, the authors proposed that the addition of Co particles, in the form of Co^{2+} and Co^0, enhanced the synthesis of C_{2+} products as it is known to be an important element for the C-C bond formation during the reaction. Also, they suggested that Cu acted as the activator of C=O bond on the surface of the catalyst, ZnO acted as promoter, improving the dispersion and stability of Cu particles, while the use of Al_2O_3, a support with Lewis acid sites, favored the methanol and di-isopropyl ether formation.

Although the array of metal combinations for the production of HAs through CO_2 hydrogenation is wide, careful consideration is needed regarding the role of each individual component, especially over the need to regulate the amount of CO and alkyl species produced. This can be achieved via combinations of transition metals, noble metals or a synergy between the two. Table 3 presents information on the catalyst formulation, reactor configuration, reaction conditions and performance in terms of CO_2 conversion and ethanol production for selected bimetallic and multimetallic systems discussed herein.

3.5. MOFs

Since the seminal work of Yaghi et al. [150], which earned the first author the moniker “the father of MOFs”, Metal–organic frameworks (MOFs), due to their ultrahigh and well-defined porosity, variable composition, structural tunability, excellent chemical stability and scalable functionality have become a family of materials widely used in adsorption, separation, and catalytic processes [151,152]. However, the only work that our literature search uncovered that utilized MOFs for the hydrogenation of CO_2 to higher alcohols was performed by An et al. [153]. Specifically, the authors utilized Zr_{12} nanoclusters as secondary building units (SBUs) and synthesized bimetallic Cu_2^I sites supported on a Zr_{12}-MOF promoted by different alkali metals (Li, Na, K, Cs). The experimental investigation was carried out in a batch reactor at $T = 100$ °C, $P = 20$ bar, H_2:$CO_2 = 3$ using tetrahydrofuran (THF) as solvent and the reported ethanol selectivity was $> 99\%$. The authors argued convincingly that this high EtOH selectivity was achieved via the synergistic action between the bimetallic Cu_2^I centers, which promote the activation of hydrogen and the direct C–C coupling of methanol and formyl species, and the alkali-metal promoters, which provide an electron-rich environment for the Cu centers to enhance activity and stabilize the formyl intermediates. Moreover, the authors also showed that the alkali metals tested affected the S_{EtOH} in the order of Li<Na<K<Cs.

3.6. Perovskite based composites

Perovskites are an interesting class of materials with applications that range from fuel cell electrodes to heterogeneous catalysts [124,154]. Their use in the hydrogenation of CO_2 to higher alcohols has been studied by Liu and co-workers [155,156]. In the first of these works [155] the authors used a series of $LaCo_{1-x}Ga_xO_3$ perovskites ($x = 0$, 0.2, 0.3, 0.4 and 0.5) and after reduction, the compositions $x = 0.2$, 0.3 and 0.4 resulted in Co/La_2O_3-$La_4Ga_2O_9$ catalysts, while $x = 0.5$ led to the $Co/La_4Ga_2O_9$ structure. The authors decided to use Ga in the system as they reasoned that it would help inhibit the hydrogenation ability of Co towards CH_4. For this purpose, they examined catalytic performance in ethanol production in a fixed bed reactor under reaction conditions of $T = 230$–290 °C, $P = 30$ bar and $H_2/CO_2 = 3.0$. Initially, the authors investigated the catalytic activity and stability of the materials during 18 h time-on-stream tests, carried out at $T = 240$ °C and as expected, the substitution of Co by Ga led to a significant decrease in the X_{CO2} and S_{CH4} and to an increase in the S_{ROH}. The selectivity to ethanol in relation to the Ga content was volcano shaped, as this improved only up to Ga= 0.3 ($LaCo_{0.7}Ga_{0.3}O_3$) and declined when the Ga concentration increased to 0.4 ($LaCo_{0.6}Ga_{0.4}O_3$); it is noted that although tested, no results regarding the alcohol distribution were provided for $LaCo_{0.5}Ga_{0.5}O_3$. The authors argued that the production of ethanol was due to presence of Ga in the perovskite matrix, which allowed the coexistence of Co^0 and $Co^{\delta+}$ on the catalyst’s interface. However, over longer time-on-stream tests (108 h) the authors observed a significant decrease in the concentration of ethanol in the products’ mix and a parallel increase in methanol, which they attributed to the oxidation of Co^0 to CoO by CO_2 and/or H_2O.

In the subsequent work [156], the authors used the $LaCo_{0.5}Ga_{0.5}O_3$ system, in order to prove that the catalytic activity observed in their previous work [155] was the result of $Co/La_4Ga_2O_9$ and not La_2O_3. The experimental work was again carried out in fixed bed reactor using $H_2/CO_2 = 3.0$, but this time the temperature under which the reaction was carried out was 270 °C and the pressure was varied from 25 to 35 bar. The authors were able to show that $La_4Ga_2O_9$ promotes mainly the RWGS producing CO, which is then hydrogenated on the Co^0 to $^*CH_x$ and on the Co^{2+} to $^*CH_xO$; following, the unhydrogenated CO or the $^*CH_xO$ species are inserted in the $^*CH_x$ species to produce ethanol.

Thus, this work showed that it is possible to synthesize an active and selective catalyst for the CO_2 to ethanol reaction by using only one active metal in different oxidation states, combining with a component responsible for catalyzing the reverse water gas shift reaction in order to generate CO species.

3.7. Zeolites

Zeolites are crystalline aluminosilicates with pores that range is size form a few angstroms to a couple of nanometers and a Si/Al ratio greater than one. This group of heterogeneous catalysts is widely used in the petrochemical industry and has been shown to have great potential in environmental catalysis [157,158]. Ding et al. [159] sought to take advantage of the properties of beta zeolite, a disordered intergrown hybrid tetragonal and clinorhombic system, and those of Cu to synthesize a catalyst for the CO_2 to ethanol hydrogenation reaction. Thus, the authors synthesized and tested a Cu@Na-Beta catalyst in a fixed-bed reactor at $T = 200$–350 °C, $P = 5$–21 bar, H_2:$CO_2 = 3$, showing an optimal ethanol and space-time yield of ~14% and ~398 $mg \cdot gcat^{-1} \cdot h^{-1}$, respectively (at 300 °C and 21 bar); importantly, the catalyst exhibited stable operation during 100 h of operation (this time $P = 13$ bar). The authors argued that the high-performance of the catalyst resulted from the successful combination and synergy of copper nanoparticles (2~5 nm) embedded into Na-Beta zeolite framework, reflecting the importance not only of the catalytic centers, but also of their surroundings.

3.8. The effect of the support

As is well understood, the interaction of the support with the active metallic component plays a crucial role in determining the activity and stability of a catalytic system. Thus, the investigation of the effect that different catalysts’ supports might have to the CO_2 hydrogenation reaction is of great importance. An interesting report along these lines has been provided by Zhang et al. [71] with the group studying the influence of Na-promoted cobalt catalysts supported on Al_2O_3 (an amphoteric oxide), ZnO and TiO_2 (oxides with oxygen vacancies), AC (a material that possesses an extremely high surface area) and SiO_2 and Si_3N_4 (inert materials) on CO_2 conversion and ethanol selectivity. Catalytic tests were performed in a fixed-bed reactor at T = 250 °C, P = 50 bar, H_2:CO_2 = 3 and catalyst activation was undertaken using CO as the reducing agent. The authors observed that during reaction CoO (which was the main phase identified on the reduced catalysts) transformed to Co_2C only on the SiO_2 and Si_3N_4 supported catalysts and to *hcp*-Co on all other systems. Given that only the SiO_2 and Si_3N_4 supported catalysts were selective towards alcohols (about 9%, while S_{ROH} for the other systems was << 1%) they concluded that Co_2C was the active phase in this system. Importantly, the authors also showed that the Co based on SiO_2 and Si_3N_4 catalysts were stable for 300 h, a behavior which they attributed to the strong-metal-support interaction (SMSI) originating from the Si-O-Co bond. This conclusion is similar to that drawn by Gnanamani et al. [121] (discussed above) who used a Na-Co/SiO_2 and showed that different reduction conditions (H_2 or syngas or CO) had an important effect on catalytic performance, and that the carburization of the Na-Co/SiO_2, which occurred under CO, helped lower the hydrogenation to methane activity of the catalyst, either through Na deposition on to Co_2C or by stabilization of the Co_2C on to the catalytic surface.

Another interesting work has been provided by Kiatphuengporn et al. [43] who used MCM-41 mesoporous silica as supporting material, due to its high surface area and ordered hexagonal structure. To investigate catalytic performance on CO_2 hydrogenation to higher alcohols production the authors synthesized Fe-doped Cu-based catalysts (xFe–10Cu), with x = 0, 0.5 and 3 wt%, utilizing unimodal (SS) and bimodal (T) MCM-41. The experimental results (fixed-bed reactor at T = 160–350 °C, P = 10 bar, H_2:CO_2 = 3) revealed that the xFe–10Cu/MCM-41 (T) catalysts with a Fe loading of 3 wt% exhibited the optimal catalytic activity with alcohol selectivity of 80–99% at T = 160–200 °C and a TOF of alcohols of $1.08 \cdot 10^{-25}$ mol surface metal atom^{-1} min^{-1}. This outstanding catalytic performance was attributed by the authors to the existence of pores with different sizes (smaller and larger mesopores) on the supporting material, which favored the HAs production by weakening the metal-support interaction, leading in turn to highly active Cu and Fe surface atoms. It can thus be concluded that the pore characteristics of the supports can influence the performance of the final catalyst towards a specific direction.

3.9. *The effect of catalyst structure*

Catalyst morphology is of great importance for the CO_2 hydrogenation reaction. As mentioned above, an early study that examined the effect of structure on performance has been provided by Li and co-workers [55,96] who, using a Pt/Co_3O_4, concluded that the specific morphology of Co_3O_4 (nanorods or nanoplates) had an important role in the reduction ability of the catalyst. Specifically, the Co_3O_4-p promoted the reduction to metallic Co at high temperatures, which favored CO_2 hydrogenation to hydrocarbons. Yang et al. [160] also investigated the relationship between the different structures, and therefore the different crystallographic planes of the catalysts and the product distribution for the reaction at hand. In particular, the authors synthesized and tested two kinds of Co-based catalysts, Co_3O_4-0 h (rhombic dodecahedra) and Co_3O_4-2 h (nanorods). Moreover, by moderating the hydrothermal time (0 h or 2 h), the authors affected the catalyst reducibility, as well as the energy requirement for the formation of oxygen vacancies. Tests were carried out in a fixed-bed reactor at T = 250–360 °C, P = 1–30 bar, H_2:CO_2 = 3 and the results revealed that the Co_3O_4-0 h catalyst was reduced to Co^0 and CoO which favors CH_4 production (S_{CH4}= 85%) while Co_3O_4-2 h reduced only to CoO which leads to CO production (S_{CO}= 95%) and therefore to alcohols formation. It was demonstrated that the selectivity of the catalyst is strongly influenced by the crystallographic planes, e.g., it was observed that CO selectivity increased when the plane changed from {111} to {110}. Also, they prepared and tested 10 wt% Cu over Co_3O_4 (0 h and 2 h) catalysts under higher pressures (1–30 bar) conditions. As the authors expected, the Cu/Co_3O_4-2 h exhibited an ethanol yield of 1.87 mmol gcat^{-1}h^{-1} almost nine time higher than Cu/Co_3O_4-0 h (0.19 mmol gcat^{-1}h^{-1}). This result was attributed to the plethora of V_O existing on Cu/Co_3O_4-0 h (111 plane) which can easily scission the *CH_3O bond and lead to methane formation. Thus, the authors were able to conclude that during the CO_2 hydrogenation the cobalt oxides with different crystallographic planes have the ability to transform into another structure and therefore regulate the product distribution.

3.10. *Tandem catalysis*

A number of literature reports [72,161–163] have tried to take advantage of tandem catalysis, a concept that was first defined by Fogg and dos Santos [164] almost 20 years ago. Simply put, in tandem catalysis the products formed during the first reaction step serve as the reactant or part of the reactant to the subsequent reaction step, thereby coupling the two reaction steps [9]. Thus, CO_2 hydrogenation for the production of HAs is an obvious example of a tandem reaction, as according to the accepted mechanism scheme, CO, produced through the RWGS reaction, is adsorbed either dissociatively or non-dissociatively and the dissociated CO* is then hydrogenated to *CH_x, which can couple with non-dissociated CO* to produce EtOH.

Chen and co-workers [72] reported a second study on the hydrogenation of CO_2 for HAs synthesis (the first, i.e., ref. [73] has been discussed above) in a fixed-bed reactor (T = 350 °C, P = 60 bar, and H_2/CO_2 = 3:1). The authors again attempted to combine a catalyst ($CuZnK_{0.15}$) known for its promoting effects on RWGS and methanol synthesis, with a catalyst ($Cu_{25}Fe_{22}Co_3K_3$) known for favoring HAs production via CO hydrogenation. However, similarly to Rahimpour et al. [165,166], who used a twin catalytic bed for methanol synthesis, the authors also used a two-stage bed catalyst system, instead of trying to combine these functions in a single catalyst. In particular, they prepared three catalyst combination systems CFCK(x)//CZK(y), CZK(y)//CFCK(x) and CFCK(x)–CZK(y), in an effort to determine the optimal loading mode (which catalyst will be placed first in the bed) and volume ratio (volume to be used from each catalytic system), reporting that the highest catalytic activity, with X_{CO2}= 32.43%, S_ROH= 11.82 wt% and STY$_R$OH= 131.0 mg mL^{-1}·h^{-1} were achieved using the CZK(1.5)//CFCK(4.5) combination. The authors concluded that ZnO helped the dispersion of Cu and that K facilitated the CuO-Zn interaction, by adjusting the transfer of surface O_2 species. Moreover, they suggested that the two-stage bed catalyst system likely aided the synthesis of HAs via a thermal coupling effect (a low-temperature RWGS catalyst with a high-temperature modified F–T synthesis catalyst) and a product conversion coupling effect.

We now turn our attention to two works produced by Hong and co-workers [161,163], a group that has been very active on the CO_2 to higher alcohols hydrogenation reaction (apart from refs. [161,163], refs. [105,108] from the same group have been discussed above). In the first of these works [161] the authors successfully combined, by powder mixing, a commercial CuZnAl catalyst, known to promote the RWGS reaction (thus, the production of CO, the key intermediary for C_{2+} synthesis) with a self-synthesized K-CuMgZnFe catalyst, known to promote the production of HAs. The experiments were conducted in a fixed-bed reactor, at T = 320 °C, P = 50 bar, and H_2/CO_2 = 3:1, the sole CuZnAl showed an S_{CO} of 90.9% and a X_{CO2} of 26.8% and no CH_4 or C_{2+} products. At the same reaction conditions, the sole K-CuMgZnFe catalyst showed a X_{CO2} of 30.4% with S_{HAs}= 15.8% and STY_{HAs}= 70.6 mg g_{cat}^{-1} h^{-1}. When the authors combined the CuZnAl with the K-CuMgZnFe, by powder mixing, in a single catalyst bed, they recorded a STY_{HAs} of 106.5 mg g_{cat}^{-1} h^{-1} with a HAs fraction of 90.2%; this result was achieved with a powder mass mixing ratio of 1:1. In the second work [163], the authors combined a system known to work for HAs synthesis, i.e., KCuFeZn with systems known to promote methanol (CH_3OH) and CO; these systems were CuZnAlZr, ZnZr and ZnCrAl. The best performing combination was that of CuZnAlZr with KCuFeZn which nearly doubled

S_{HAs} and STY compared to the use of the sole KCuFeZn (S_{HAs} rose from 17.4% to 33% and STY_{HAs} increased from 42.1 $mg \cdot g_{cat}^{-1} \cdot h^{-1}$ to 84.0 $mg \cdot g_{cat}^{-1} \cdot h^{-1}$). Thus, in this way, the authors were able to show that extra $*CH_xO$/*CO species have a key role to play for the reaction at hand.

Finally, Tsubaki and co-workers [162] combined a catalyst able to produce alkenes, Na-Fe@C, with a catalyst known to work on HAs synthesis, K-CuZnAl; the weight ratio used was 1:1 and the catalytic performance tests were carried out in a fixed-bed reactor at T = 320 °C, P = 50 bar, and $H_2/CO_2 \sim$ 3:1. The authors reported a CO_2 conversion of 39.2% and an ethanol selectivity of 35%, which compares very favorably with the literature [72,75,78,102,118], and via in-situ characterizations and DFT calculations concluded that the catalytic interfaces, achieved by the combination of these catalytic systems, and the formation of intermediate aldehyde species were responsible for these excellent results.

Table 4 presents information on the catalyst formulation, reactor configuration, reaction conditions and performance in terms of CO_2 conversion and ethanol production for tandem catalytic systems discussed herein.

4. Mechanistic studies

Concerning the reaction mechanism, two main approaches have been reported in the literature. The first approach, and based on the existing studies the most widely accepted, is that the HAs synthesis proceeds via a CO-mediated pathway; this mechanism was first put forward by Kusama et al. [75,76], using a Rh-Fe/SiO_2 catalyst. Specifically, this mechanism involves the following steps: (i) CO is formed through the RWGS reaction; (ii) the dissociative adsorption of CO leads to the formation of alkyl species ($*C_xH_y$) and the non-dissociative adsorption of CO leads to its insertion into the alkyl species ($*C_xH_yCO$); (iii) hydrogenation of the latter (i.e., $*C_xH_yCO$) then leads to the desired higher alcohols (e.g., $C_xH_yCH_2OH$). Hong and co-workers [105] investigated the origins of alkyl species for the CO insertion mechanism over Cs-modified CuFeZn (CFZ) catalysts. They conducted a methanol steam reforming experiment under H_2 flow in order to reveal the possibility of methanol C-O bond cleavage over the studied catalyst. From the received products (CO_2, CO) as well as from in-situ DRIFTS experiments, they concluded that the $*CH_3$ formation is a result of hydrogenation of dissociated CO (Fig. 13).

In a similar way, Yao et al. [127] discussed above, studying the influence of different Fe sites on the surface of a FeNaS catalyst reported that *CO dissociation and conversion to $*CH_x$ and other hydrocarbon moieties was favored when Fe was away from S atoms, while the latter could modulate the $*CH_x$–*CO coupling reaction. As a final example, Limtrakul and his co-workers [141], using KCo-In_2O_3, also proposed a CO-mediated pathway. Specifically, the authors argued that the support (In_2O_3) provided oxygen vacancies over which the RWGS reaction produced CO and that Co^0 was responsible for the dissociative adsorption of CO, the growth of the C-C chain and the production of $*C_xH_y$ through the hydrogenation of the adsorbed carbon. The non-dissociative CO migrated from the CoO sites to Co^0 in order to couple with $*C_xH_y$ species to form HAs (Fig. 11).

The second approach, originally proposed by He et al. [95] using Pt/Co_3O_4 catalysts, proceeds via a methoxy-mediated pathway. Specifically, after carrying out labelling experiments, the authors were able to show that H_2O also participates in the reaction, which led them to propose that the production of ethanol proceeds via a methanol-intermediated mechanism in which the H that results from the dissociation of H_2O can protonate the produced methanol. This in turn can dissociate into $*CH_3$, *OH, and *H, with $*CH_3$ then being able to couple with CO to form $*CH_3CO$, which finally produces ethanol via its further hydrogenation. Similarly, Ding et al. [159], testing a Cu@Na-Beta catalyst, proposed an acetate/methoxy-mediated pathway. Specifically, the authors proposed that CO_2 is hydrogenated to $*CH_3O$ and/or $*CH_3OH$ on the surface of the catalyst either through the RWGS reaction and the hydrogenation of the produced *CO or hydrogenation of $*CO_2$ to formate (*HCOO) followed by its hydrogenation and dissociation to methoxy or methanol. $*CH_3O$ (Eq. 4) and/or $*CH_3OH$ (Eq. 5) in turn scission to form $*CH_3$ species. Then, through the C-C coupling reaction of $*CO_2$ with $*CH_3$ or $*CH_3O$ acetate species ($*CH_3COO$) are formed and finally, the $*CH_3COO$ species undergo additional hydrogenation to produce ethanol (Eqs. 6 and 7) [159].

$$*CH_3O \rightarrow *CH_3 + *O \tag{4}$$

$$*CH_3OH \rightarrow *CH_3 + *OH \tag{5}$$

$$*CO_2 + *CH_3 + 2\,H_2 \rightarrow *CH_3CH_2OH + *OH \tag{6}$$

$$*CO_2 + *CH_3O + 2\,H_2 \rightarrow *CH_3CH_2OH + *O + *OH \tag{7}$$

Liu and co-workers [155], using a Co/La_2O_3-$La_4Ga_2O_9$ catalyst, suggested a formate/methoxy pathway. Specifically, the authors argued that the dissociated and non-dissociated $*CO_2$ reacts with hydrogen atoms to form $*CH_3$ and *HCOO species, respectively. The latter can be decomposed into *CO followed by its coupling with $*CH_3$ species to form $*CH_3CO$ species. EtOH can then be synthesized from the hydrogenation of $*CH_3CO$.

It is noted that, the $*CH_x$ species produced during the CO_2 hydrogenation reaction, apart from $*CH_x$ – *CO coupling to form C_{2+}

Table 4
Composition, synthesis technique, experimental conditions and performance of catalysts as reported in selected works of tandem catalysis from the literature.

Catalyst	Synthesis method	Experimental conditions	Catalytic activity	Ref.
CZK(x)//CFCK(y) (loading volume: x = 1.5, y = 4.5) (CZK: $CuZn_{1.0}K_{0.15}$ CFCK:$Cu_{25}Fe_{22}Co_3K_3$)	K/Cu–Zn catalysts were prepared by co-precipitation impregnation method and CFCK were prepared by impregnation method	fixed-bed reactor, T = 350 °C, P = 60 bar, H_2/CO_2 = 3, GHSV= 5000 h^{-1}	X_{CO2}= 32.43% S_ROH= 11.82% STY_ROH= 131.0 mg $mL^{-1} \cdot h^{-1}$ $C_{2+}OH/C_1OH$= 1.24	[72]
CuZnAl with K-CuMgZnFe (mass mixing ratio of 1:1)	K-CMZF catalysts were prepared by a coprecipitation method and mixed with commercial CuZA catalyst	fixed-bed reactor, T = 320 °C, P = 50 bar, H_2/CO_2 = 3, GHSV= 6000 mL g_{cat}^{-1} h^{-1}	X_{CO2}= 42.3% S_{Et}OH= 17.4% STY_{HA}s = 106.5 mg g_{cat}^{-1} h^{-1} $C_{2+}OH/ROH$= 90.2 wt%	[161]
CuZnAlZr with 4.7KCuFeZn (1:1-powder mixing)	Both K–Cu–Fe–Zn and Cu–Zn–Al–Zr catalysts were prepared by a coprecipitation method	fixed-bed reactor, T = °C, P = 50 bar, H_2/CO_2 = 3, GHSV= 3000 mL g_{cat}^{-1} h^{-1}	S_{HA}= 33% STY_{HAs}= 84.0 $mg \cdot g_{cat}^{-1} \cdot h^{-1}$	[163]
2%Na-Fe@C with 5%K-CuZnAl (weight ratio= 1:1)	Fe@C catalysts were prepared by pyrolyzing the Fe-MOFs which were prepared by a hydrothermal method. CuZnAl catalysts were prepared by precipitation method.	fixed-bed reactor at T = 320 °C, P = 50 bar, and H_2/CO_2 = 2.65	X_{CO2}= 39.2% S_{Et}OH= 35% S_{Pr}OH= 4.0% S_{Bt}OH= 1.2% S_{C5}= 0.7% Y_{Et}OH= 12.4%	[162]

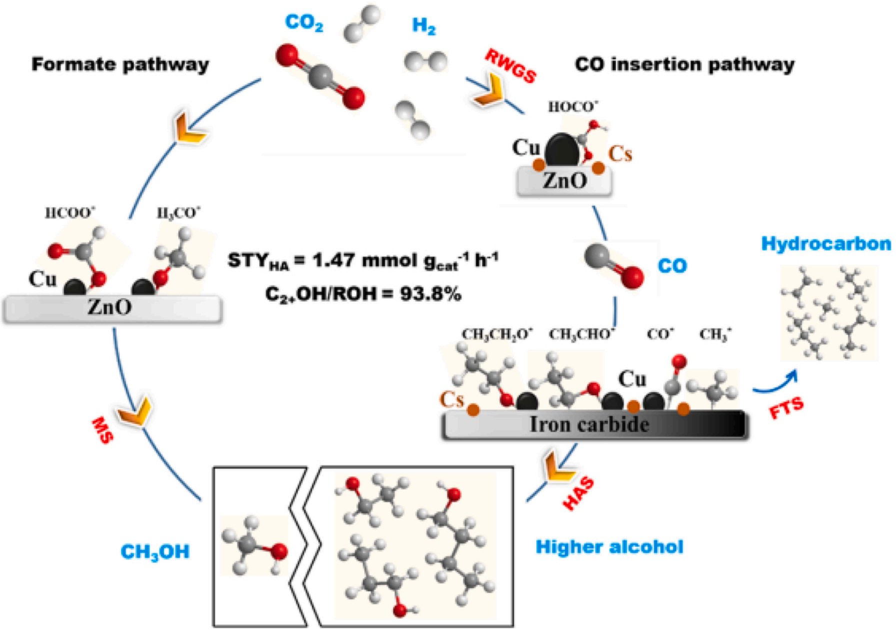

Fig. 13. Schematic representation of the reaction pathway followed over Cs-CuFeZn catalysts during CO_2 hydrogenation [105].

alcohols, can undergo different additional possible reactions leading to a plethora of by-products (alkanes, alkenes, alcohols), as shown in the below reaction scheme [108].

$^*CH_x + {^*H} \rightarrow CH_4$ ($^*CH_x$ termination by hydrogenation) (8)

$2^*CH_x \rightarrow C_2H_4$ ($^*CH_x$-$^*CH_x$ coupling) (9)

$2^*CH_x + {^*H} \rightarrow C_2H_6$ ($^*CH_x$-$^*CH_x$ coupling and termination by hydrogenation) (10)

$^*CH_x + {^*CO} + {^*H} \rightarrow C_2H_5OH$ ($^*CH_x$-$^*CO$ coupling and termination by hydrogenation) (11)

Thus, the discussion above over the prevailing mechanistic theories makes clear that although there have been many efforts in exploring the mechanism of C_{2+} production via CO_2 hydrogenation, our mechanistic knowledge is yet at an early stage due to the greater complexity of reaction pathways in comparison with the well-studied mechanism of C_1 production.

5. Conclusions and future perspectives

Higher alcohol (HA) synthesis via the hydrogenation of CO_2 constitutes a relatively new and exciting field of research that has the potential to help towards the de-carbonization of the energy sector. The review paper presented herein provides a comprehensive and critical literature review of the catalytic formulations that have been employed, in both fixed-bed and batch reactors, and of the critical role of promoters and supports and discusses the thermodynamic aspects of the reaction and the insights that have been gained regarding the reaction mechanism.

Succinctly, various noble metal catalysts appropriately modified have been shown to be active in producing HAs via CO_2 hydrogenation. For example, Rh-based catalysts modified by the addition of an alkali metal (Li or K) and/or Fe have been shown to increase the amount of the CO intermediates, which then react with $^*CH_3$ to form ethanol. Alkali metals help lower the production of alkanes via the hydrogenation of the intermediates (C_xH_y), which improves HAs synthesis, lower the production of methanol and balance the active sites that are responsible for the dissociation and non-dissociation of CO. Moreover, the use of supporting materials with a high population of oxygen vacancies is beneficial to the reaction, as they help tune the metal-support-interaction and activate the CO_2 molecule.

Regarding transition metal-based catalysts, alkali modified Cu/ZnO/Fe catalysts are the standout candidates, as they have been shown to be active in producing HAs via CO_2 hydrogenation. These systems combine the methanol synthesis capability of Cu/Zn with the RWGS reaction activity of Fe, but it is important to balance the FeC_x species, which promote the dissociation of CO, the C-C chain growth and the hydrogenation reaction, and Cu species, which promote the non-dissociation of CO. Co-based catalysts on the other hand exhibit relatively low CO_2 conversion and HAs selectivity, with their performance being highly dependent on the formation of Co^0, CoO, $Co^{\delta+}$ and Co_2C and the synergy between these species. These Co hetero sites depend on the reduction process, the presence of alkali metals and the interaction between Co and the supports/promoters. However, Co has been successfully used as promoter in In_2O_3 based systems or in combination with another metal (e.g., Fe or Cu) in bimetallic/multimetallic catalyst formulations. Finally, the Mo-based catalysts tested so far have not been shown to be successful in making the shift from methanol and CO production to C_{2+} alcohols.

The literature review that we have carried out shows that the high specific activity achieved using single atom catalysts holds great promise for the production of HAs via the hydrogenation of CO_2, as these systems appear capable of aiding the successful cleavage of the C=O bond and the preferential formation of a C-C bond. The SACs systems reported so far also clearly show the benefits of using oxides with abundant oxygen vacancies. Moreover, as by definition, SACs provide highly dispersed metal species, such catalysts can be cost effective alternatives to their nanoparticle and sub-nanometer clusters counterparts.

Core-shell structured catalysts is another family of materials that should be considered for the production of HAs through CO_2 hydrogenation. Such catalysts constitute a relatively new family of materials which have already been shown to provide advantages in CO_2 conversion reactions (e.g., reforming of methane, hydrogenation to CO, CH_4, methanol, C_{2+} hydrocarbons and oxygenates). For instance, their structure promotes the interaction between the different catalytic components, enhancing their bifunctionality, a property which is significant for $C_{2+}OH$ production. We hypothesize that in a typical core-shell catalyst, the metal of the core is likely to promote the RWGS reaction producing CO, while the outer shell could promote the FTS reaction producing alkyl species which then could react with the produced

CO towards $C_{2+}OH$.

Tandem catalysis also seems to hold great promise in HAs synthesis through CO_2 hydrogenation, as according to the accepted mechanism scheme, CO, produced through the RWGS reaction, is adsorbed either dissociatively or non-dissociatively and the dissociated CO* is then hydrogenated to *CH_x, which can couple with non-dissociated CO* to produce EtOH. Research on such systems focuses not only on finding the appropriate catalytic systems, but also on the powder mass mixing ratio, loading mode and volume ratio.

Regarding the understanding of the reaction mechanism, the current state of understanding is yet at an early stage, due to the great complexity of reaction pathways, especially in comparison with the well-studied mechanism of C_1 production. In general, it is thought that the reaction proceeds either through a CO- or a methanol-mediated pathway however, efforts to verify the precise mechanism, employing computational chemistry and in-situ or operando techniques should be intensified. In this direction the use of artificial intelligence, may also prove useful.

Future research efforts should also be directed towards investigating the in-situ methanol homologation reaction. The term “homologation” refers to a reaction in which a molecule is transformed to a product by the addition of a carbon atom, to form a C-C bond, and as methanol production via CO_2 hydrogenation is already well established, it might be possible to couple methanol-methanol to form the desired HAs. Moreover, the synthesis of new bifunctional catalysts capable of producing and transforming dimethyl ether (DME) to $C_{2+}OH$ may also be worthy of investigation.

At the same time, in addition to tailoring and optimizing the catalytic materials for the selective production of higher alcohols it is clear that the operating parameters such as temperature and pressure and the ratio of hydrogen to carbon dioxide should be carefully considered, as they have an important effect on performance and selectivity. Moreover, in batch reactors, it is important to also use an appropriate solvent. Research towards this direction shows that polar, protic solvents should be preferred as these have the ability to donate protons and aid the production of HAs. However, the choice of solvent should also be made keeping in mind the need to design an integrated process in line with the principles of green chemistry and circular economy. Lastly, the coupling of catalytic HAs production with electromagnetic radiation (such as microwaves, ultrasound or an integrated photothermal process) may potentially increase selectivity and efficiency at milder operating conditions.

CRediT authorship contribution statement

Angeliki I. Latsiou: Conceptualization, Methodology, Validation, Investigation, Writing – original draft. **Nikolaos D. Charisiou:** Investigation, Writing – review & editing, Supervision, Project administration. **Zacharias Frontistis:** Writing – review & editing. **Atul Bansode:** Writing – review & editing. **Maria A. Goula:** Conceptualization, Writing – review & editing, Supervision, Project administration, Funding acquisition.

Declaration of Competing Interest

The authors declare that they have no known competing financial interests or personal relationships that could have appeared to influence the work reported in this paper.

Data Availability

Data will be made available on request.

Acknowledgements

The authors gratefully acknowledge support of this work by the project “Development of new innovative low carbon energy technologies to improve excellence in the Region of Western Macedonia” (MIS 5047197) which is implemented under the Action “Reinforcement of the Research and Innovation Infrastructure” funded by the Operational Program "Competitiveness, Entrepreneurship and Innovation" (NSRF 2014-2020) and co-financed by Greece and the European Union (European Regional Development Fund).

References

[1] Global Climate Change, Carbon Dioxide. ⟨https://climate.nasa.gov/vital-signs/carbon-dioxide/⟩ (accessed 6/04/2022) 20.

[2] SRES refers to the IPCC Special Report on Emission Scenarios (2000) (⟨https://www.climate.gov/news-features/understanding-climate/climate-change-global-temperature-projections⟩).

[3] R.-P. Ye, J. Ding, W. Gong, M.D. Argyle, Q. Zhong, Y. Wang, C.K. Russell, Z. Xu, A.G. Russell, Q. Li, M. Fan, Y.G. Yao, CO_2 hydrogenation to high-value products via heterogeneous catalysis, Nat. Commun. 10 (2019) 5698, https://doi.org/10.1038/s41467-019-13638-9.

[4] C. Panzone, R. Philippe, A. Chappaz, P. Fongarland, A. Bengaouer, Power-to-Liquid catalytic CO_2 valorization into fuels and chemicals: focus on the Fischer-Tropsch route, *J. CO_2 Util.* 38 (2020) 314–347, https://doi.org/10.1016/j.jcou.2020.02.009.

[5] A.D.N. Kamkeng, M. Wang, J. Hu, W. Du, F. Qian, Transformation technologies for CO_2 utilisation: current status, challenges and future prospects, Chem. Eng. J. 409 (2021), 128138, https://doi.org/10.1016/j.cej.2020.128138.

[6] O. Elishav, Y. Shener, V. Beilin, M.V. Landau, M. Herskowitz, G.E. Shter, G. S. Grader, Electrospun Fe–Al–O Nanobelts for Selective CO_2 Hydrogenation to Light Olefins, ACS Appl. Mater. Inter. 12 (2020) 24855–24867, https://doi.org/10.1021/acsami.0c05765.

[7] O.A. Ojelade, S.F. Zaman, A review on CO_2 hydrogenation to lower olefins: understanding the structure-property relationships in heterogeneous catalytic systems, J. CO_2 Util. 47 (2021), 101506, https://doi.org/10.1016/j.jcou.2021.101506.

[8] W. Li, K. Wang, G. Zhan, J. Huang, Q. Li, Design and synthesis of bioinspired $ZnZrO_x$&Bio-ZSM-5 integrated nanocatalysts to boost CO_2 hydrogenation to light olefins, ACS Sust. Chem. Eng. 9 (2021) 6446–6458, https://doi.org/10.1021/acssuschemeng.1c01384.

[9] Y. Gambo, S. Adamu, R.A. Lucky, M.S. Ba-Shammakh, M.M. Hossain, Tandem catalysis: a sustainable alternative for direct hydrogenation of CO_2 to light olefins, Appl. Catal. A: Gen. 641 (2022), 118658, https://doi.org/10.1016/j.apcata.2022.118658.

[10] P. Tian, G. Zhan, J. Tian, K.B. Tan, M. Guo, Y. Han, T. Fu, J. Huang, Q. Li, Direct CO_2 hydrogenation to light olefins over $ZnZrO_x$ mixed with hierarchically hollow SAPO-34 with rice husk as green silicon source and template, Appl. Catal. B: Environ. 315 (2022), 121572, https://doi.org/10.1016/j.apcatb.2022.121572.

[11] L. Shen, J. Xu, M. Zhu, Y.-F. Han, Essential role of the support for nickel-based CO_2 methanation catalysts, ACS Catal. 10 (2020) 14581–14591, https://doi.org/10.1021/acscatal.0c03471.

[12] F. Botzolaki, G. Goula, A. Rontogianni, E. Nikolaraki, N. Chalmpes, P. Zygouri, M. Karakassides, D. Gournis, N.D. Charisiou, M.A. Goula, S. Papadopoulos, I. V. Yentekakis, CO_2 methanation on supported Rh nanoparticles: the combined effect of support oxygen storage capacity and Rh particle size, Catalysts 10 (2020) 944, https://doi.org/10.3390/catal10080944.

[13] G.I. Siakavelas, N.D. Charisiou, A. AlKhoori, S. AlKhoori, V. Sebastian, S. J. Hinder, M.A. Baker, I.V. Yentekakis, K. Polychronopoulou, M.A. Goula, Highly selective and stable Ni/La-M (M=Sm, Pr, and Mg)-CeO_2 catalysts for CO_2 methanation, *J. CO_2 Util.* 51 (2021), 101618, https://doi.org/10.1016/j.jcou.2021.101618.

[14] G.I. Siakavelas, N.D. Charisiou, S. AlKhoori, A.A. AlKhoori, V. Sebastian, S. J. Hinder, M.A. Baker, I.V. Yentekakis, K. Polychronopoulou, M.A. Goula, Highly selective and stable nickel catalysts supported on ceria promoted with Sm_2O_3, Pr_2O_3 and MgO for the CO_2 methanation, Appl. Catal. B: Environ. 282 (2021), 119562, https://doi.org/10.1016/j.apcatb.2020.119562.

[15] W.K. Fan, M. Tahir, Recent trends in developments of active metals and heterogenous materials for catalytic CO_2 hydrogenation to renewable methane: a review, J. Environ. Chem. Eng. 9 (2021), 105460, https://doi.org/10.1016/j.jece.2021.105460.

[16] A.I. Tsiotsias, N.D. Charisiou, E. Harkou, S. Hafeez, G. Manos, A. Constantinou, A. G.S. Hussien, A.A. Dabbawala, V. Sebastian, S.J. Hinder, M.A. Baker, K. Polychronopoulou, M.A. Goula, Enhancing CO_2 methanation over Ni catalysts supported on sol gel derived Pr_2O_3-CeO_2: An experimental and theoretical investigation, Appl. Catal. B: Environ. 318 (2022), 121836, https://doi.org/10.1016/j.apcatb.2022.121836.

[17] A.I. Tsiotsias, N.D. Charisiou, A. AlKhoori, S. Gaber, V. Stolojan, V. Sebastian, B. van der Linden, A. Bansode, S.J. Hinder, M.A. Baker, K. Polychronopoulou, M. A. Goula, Optimizing the oxide support composition in Pr-doped CeO_2, towards highly active and selective Ni-based CO_2 methanation catalysts, J. Energ. Chem. 71 (2022) 547–561, https://doi.org/10.1016/j.jechem.2022.04.003.

[18] P. Verma, S. Zhang, S. Song, K. Mori, Y. Kuwahara, M. Wen, H. Yamashita, T. An, Recent strategies for enhancing the catalytic activity of CO_2 hydrogenation to formate/formic acid over Pd-based catalyst, *J. CO_2 Util.* 54 (2021), 101765, https://doi.org/10.1016/j.jcou.2021.101765.

[19] X. Hu, M. Luo, M. ur Rehman, J. Sun, H.A.S.M. Yaseen, F. Irshad, Y. Zhao, S. Wang, X. Ma, Mechanistic insight into the electron-donation effect of modified ZIF-8 on Ru for CO_2 hydrogenation to formic acid, *J. CO_2 Util.* 60 (2022), 101992, https://doi.org/10.1016/j.jcou.2022.101992.

[20] Li.D. Naimatullah, G. Gahungu, W. Li, J. Zhang, First-principles calculations on CO_2 hydrogenation to formic acid over a metal-doped boron phosphide, Mol. Catal. 527 (2022), 112412, https://doi.org/10.1016/j.mcat.2022.112412.

[21] Y. Zhang, Y. Mo, Z. Cao, Rational design of main group metal-embedded nitrogen-doped carbon materials as frustrated lewis pair catalysts for CO_2 hydrogenation to formic acid, ACS Appl. Mater. Inter. 14 (2022) 1002–1014, https://doi.org/10.1021/acsami.1c20230.

[22] X.-X. Hou, C.-H. Xu, Y.-L. Liu, J.-J. Li, X.-D. Hu, J. Liu, J.-Y. Liu, Q. Xu, Improved methanol synthesis from CO_2 hydrogenation over CuZnAlZr catalysts with precursor pre-activation by formaldehyde, J. Catal. 379 (2019) 147–153, https://doi.org/10.1016/j.jcat.2019.09.025.

[23] H. Ham, S.W. Baek, C.-H. Shin, J.W. Bae, Roles of structural promoters for direct CO_2 hydrogenation to dimethyl ether over ordered mesoporous bifunctional Cu/M–Al_2O_3 (M = Ga or Zn), ACS Catal. 9 (2019) 679–690, https://doi.org/10.1021/acscatal.8b04060.

[24] S. Ren, W.R. Shoemaker, X. Wang, Z. Shang, N. Klinghoffer, S. Li, M. Yu, X. He, T. A. White, X. Liang, Highly active and selective Cu-ZnO based catalyst for methanol and dimethyl ether synthesis via CO_2 hydrogenation, Fuel 239 (2019) 1125–1133, https://doi.org/10.1016/j.fuel.2018.11.105.

[25] Q. Sheng, R.-P. Ye, W. Gong, X. Shi, B. Xu, M. Argyle, H. Adidharma, M. Fan, Mechanism and catalytic performance for direct dimethyl ether synthesis by CO_2 hydrogenation over CuZnZr/ferrierite hybrid catalyst, J. Environ. Sci. 92 (2020) 106–117, https://doi.org/10.1016/j.jes.2020.02.015.

[26] W. Yue, Z. Wan, Y. Li, X. He, J. Caro, A. Huang, Synthesis of Cu–ZnO–Pt@HZSM-5 catalytic membrane reactor for CO_2 hydrogenation to dimethyl ether, J. Membr. Sci. 660 (2022), 120845, https://doi.org/10.1016/j.memsci.2022.120845.

[27] B. Tidona, C. Koppold, A. Bansode, A. Urakawa, P. Rudolf Von Rohr, CO_2 hydrogenation to methanol at pressures up to 950 bar, J. Supercrit. Fluid. 78 (2013) 70–77, https://doi.org/10.1016/j.supflu.2013.03.027.

[28] A. Bansode, A. Urakawa, Towards full one-pass conversion of carbon dioxide to methanol and methanol-derived products, J. Catal. 309 (2014) 66–70, https://doi.org/10.1016/j.jcat.2013.09.005.

[29] C. Meng, G. Zhao, X.-R. Shi, Q. Nie, Y. Liu, Y. Lu, Electronic modulation of $InNi_3C_{0.5}/Fe_3O_4$ by support precursor toward efficient CO_2 hydrogenation to methanol, Appl. Catal. B: Environ. 316 (2022), 121699, https://doi.org/10.1016/j.apcatb.2022.121699.

[30] Y. Zhang, Y. He, M. Cao, B. Liu, J. Li, High selective methanol synthesis from CO_2 hydrogenation over Mo-Co-C-N catalyst, Fuel 325 (2022), 124854, https://doi.org/10.1016/j.fuel.2022.124854.

[31] F. Zeng, C. Mebrahtu, X. Xi, L. Liao, J. Ren, J. Xie, H.J. Heeres, R. Palkovits, Catalysts design for higher alcohols synthesis by CO_2 hydrogenation: Trends and future perspectives, Appl. Catal. B: Environ. 291 (2021), 120073, https://doi.org/10.1016/j.apcatb.2021.120073.

[32] D. Xu, Y. Wang, M. Ding, X. Hong, G. Liu, S.C.E. Tsang, Advances in higher alcohol synthesis from CO_2 hydrogenation, Chem 7 (2021) 849–881, https://doi.org/10.1016/j.chempr.2020.10.019.

[33] P. Gao, L. Zhang, S. Li, Z. Zhou, Y. Sun, Novel heterogeneous catalysts for CO_2 hydrogenation to liquid fuels, ACS Cent. Sci. 6 (2020) 1657–1670, https://doi.org/10.1021/acscentsci.0c00976.

[34] S. Zhang, Z. Wu, X. Liu, K. Hua, Z. Shao, B. Wei, C. Huang, H. Wang, Y. Sun, A short review of recent advances in direct CO_2 hydrogenation to alcohols, Top. Catal. 64 (2021) 371–394, https://doi.org/10.1007/s11244-020-01405-w.

[35] S. Liu, Y. He, W. Fu, J. Chen, J. Ren, L. Liao, R. Sun, Z. Tang, C. Mebrahtu, F. Zeng, Hetero-site cobalt catalysts for higher alcohols synthesis by CO_2 hydrogenation: A review, J. CO_2 Util. 67 (2023), 102322, https://doi.org/10.1016/j.jcou.2022.102322.

[36] S. Schemme, J.L. Breuer, R.C. Samsun, R. Peters, D. Stolten, Promising catalytic synthesis pathways towards higher alcohols as suitable transport fuels based on H_2 and CO_2, J. CO_2 Util. 27 (2018) 223–237, https://doi.org/10.1016/j.jcou.2018.07.013.

[37] S. Liu, H. Zhou, Q. Song, Z. Ma, Synthesis of higher alcohols from CO_2 hydrogenation over Mo–Co–K sulfide-based catalysts, J. Taiwan Inst. Chem. Eng. 76 (2017) 18–26, https://doi.org/10.1016/j.jtice.2017.04.007.

[38] X. Wang, P.J. Ramírez, W. Liao, J.A. Rodriguez, P. Liu, Cesium-induced active sites for C−C coupling and ethanol synthesis from CO_2 hydrogenation on Cu/ZnO $(000\bar{1})$ surfaces, J. Am. Chem. Soc. 143 (2021) 13103–13112, https://doi.org/10.1021/jacs.1c03940.

[39] E. Erdiwansyah, R. Mamat, M.S.M. Sani, K. Sudhakar, A. Kadarohman, R. E. Sardjono, An overview of higher alcohol and biodiesel as alternative fuels in engines, Energy Rep. 5 (2019) 467–479, https://doi.org/10.1016/j.egyr.2019.04.009.

[40] F.A. Rahman, M.M.A. Aziz, R. Saidur, W.A.W.A. Bakar, M.R. Hainin, R. Putrajaya, N.A. Hassan, Pollution to solution: Capture and sequestration of carbon dioxide (CO_2) and its utilization as a renewable energy source for a sustainable future, Renew. Sust. Energ. Rev. 71 (2017) 112–126, https://doi.org/10.1016/j.rser.2017.01.011.

[41] R.G. Herman, Advances in catalytic synthesis and utilization of higher alcohols, Catal. Today 55 (2000) 233–245, https://doi.org/10.1016/S0920-5861(99)00246-1.

[42] H.T. Luk, C. Mondelli, D.C. Ferré, J.A. Stewart, J. Pérez-Ramírez, Status and prospects in higher alcohols synthesis from syngas, Chem. Soc. Rev. 46 (2017) 1358–1426, https://doi.org/10.1039/C6CS00324A.

[43] S. Kiatphuengporn, M. Chareonpanich, J. Limtrakul, Effect of unimodal and bimodal MCM-41 mesoporous silica supports on activity of Fe–Cu catalysts for CO_2 hydrogenation, Chem. Eng. J. 240 (2014) 527–533, https://doi.org/10.1016/j.cej.2013.10.090.

[44] H.B. Aditiya, T.M.I. Mahlia, W.T. Chong, Hadi Nur, A.H. Sebayang, Second generation bioethanol production: a critical review, Renew. Sust. Energ. Rev. 66 (2016) 631–653, https://doi.org/10.1016/j.rser.2016.07.015.

[45] A. Bušić, N. Marđetko, S. Kundas, G. Morzak, H. Belskaya, M.I. Šantek, D. Komes, S. Novak, B. Šantek, Bioethanol Production from Renewable Raw Materials and Its Separation and Purification: A Review, Food Technol. Biotechnol. 56 (2018) 289–311, https://doi.org/10.17113/ftb.56.03.18.5546.

[46] Z. Zhang, T. Mamba, E. Yamamoto, H. Murayama, T. Ishida, T. Honma, T. Fujitani, M. Tokunaga, Direct transformation of terminal alkenes with H_2O into primary alcohols over metal oxide-supported Pd catalysts, Appl. Catal. B: Environ. 246 (2019) 100–110, https://doi.org/10.1016/j.apcatb.2019.01.031.

[47] D.J. Nelson, C. Brammer, R. Li, Substituent effects in acid-catalyzed hydration of alkenes, measured under consistent reaction conditions, Tetrahedron Lett. 50 (2009) 6454–6456, https://doi.org/10.1016/j.tetlet.2009.08.128.

[48] X. Hu, G. Zhang, F. Bu, A. Lei, Visible-light-mediated anti-markovnikov hydration of olefins, ACS Catal. 7 (2017) 1432–1437, https://doi.org/10.1021/acscatal.6b03388.

[49] Y. Xiang, R. Barbosa, N. Kruse, Higher alcohols through CO hydrogenation over CoCu catalysts: influence of precursor activation, ACS Catal. 4 (2014) 2792–2800, https://doi.org/10.1021/cs500696z.

[50] W.U. Khan, L. Baharudin, J. Choi, A.C.K. Yip, Recent progress in CO hydrogenation over bimetallic catalysts for higher alcohol synthesis, ChemCatChem 13 (2021) 111–120, https://doi.org/10.1002/cctc.202001436.

[51] M. Ao, G.H. Pham, J. Sunarso, M.O. Tade, S. Liu, Active centers of catalysts for higher alcohol synthesis from syngas: a review, ACS Catal. 8 (2018) 7025–7050, https://doi.org/10.1021/acscatal.8b01391.

[52] E. Heracleous, E.T. Liakakou, A.A. Lappas, A.A. Lemonidou, Investigation of K-promoted Cu-Zn-Al, Cu-X-Al and Cu-Zn-X (X= Cr, Mn) catalysts for carbon monoxide hydrogenation to higher alcohols, Appl. Catal. A: Gen. 455 (2013) 145–154, https://doi.org/10.1016/j.apcata.2013.02.001.

[53] P. Borisut, A. Nuchitprasittichai, Methanol production via CO_2 hydrogenation: sensitivity analysis and simulation—based optimization, Front. Energy Res. 7 (2019) 81, https://doi.org/10.3389/fenrg.2019.00081.

[54] S. Hafeez, E. Harkou, S.M. Al-Salem, M.A. Goula, N. Dimitratos, N.D. Charisiou, A. Villa, A. Bansode, G. Leeke, G. Manos, A. Constantinou, Hydrogenation of carbon dioxide (CO_2) to fuels in microreactors: a review of set-ups and value-added chemicals production, React. Chem. Eng. 7 (2022) 795–812, https://doi.org/10.1039/D1RE00479D.

[55] X. Nie, W. Li, X. Jiang, X. Guo, C. Song, Chapter two - recent advances in catalytic CO_2 hydrogenation to alcohols and hydrocarbon, Adv. Catal. 65 (2019) 121–233, https://doi.org/10.1016/bs.acat.2019.10.002.

[56] B. Liu, B. Ouyang, Y. Zhang, K. Lv, Q. Li, Y. Ding, J. Li, Effects of mesoporous structure and Pt promoter on the activity of Co-based catalysts in low-temperature CO_2 hydrogenation for higher alcohol synthesis, J. Catal. 366 (2018) 91–97, https://doi.org/10.1016/j.jcat.2018.07.019.

[57] Y. He, S. Liu, W. Fu, C. Wang, C. Mebrahtu, R. Sun, F. Zeng, Thermodynamic analysis of CO_2 hydrogenation to higher alcohols ($C_{2\text{–}4}OH$): effects of isomers and methane, ACS Omega 7 (2022) 16502–16514, https://doi.org/10.1021/acsomega.2c00502.

[58] R. Guil-López, N. Mota, J. Llorente, E. Millán, B. Pawelec, J.L.G. Fierro, R. M. Navarro, Methanol synthesis from CO_2: a review of the latest developments in heterogeneous catalysis, Materials 12 (2019) 3902, https://doi.org/10.3390/ma12233902.

[59] T. Biswal, K.P. Shadangi, P.K. Sarangi, R.K. Srivastava, Conversion of carbon dioxide to methanol: a comprehensive review, Chemosphere 298 (2022), 134299, https://doi.org/10.1016/j.chemosphere.2022.134299.

[60] M.D. Garba, M. Usman, S. Khan, F. Shehzad, A. Galadima, M.F. Ehsan, A. S. Ghanem, M. Humayun, CO_2 towards fuels: a review of catalytic conversion of carbon dioxide to hydrocarbons, J. Environ. Chem. Eng. 9 (2021), 104756, https://doi.org/10.1016/j.jece.2020.104756.

[61] L. Cui, C. Liu, B. Yao, P.P. Edwards, T. Xiao, F. Cao, A review of catalytic hydrogenation of carbon dioxide: From waste to hydrocarbons, Front. Chem. 10 (2022) 1037997, https://doi.org/10.3389/fchem.2022.1037997.

[62] M. Zhu, Q. Ge, X. Zhu, Catalytic reduction of CO_2 to CO via reverse water gas shift reaction: recent advances in the design of active and selective supported metal catalysts, Trans. Tianjin Univ. 26 (2020) 172–187, https://doi.org/10.1007/s12209-020-00246-8.

[63] A.M. Bahmanpour, M. Signorile, O. Kröcher, Recent progress in syngas production via catalytic CO_2 hydrogenation reaction, Appl. Catal. B: Environ. 295 (2021), 120319, https://doi.org/10.1016/j.apcatb.2021.120319.

[64] W.-J. Shen, K.-W. Jun, H.-S. Choi, K.-W. Lee, Thermodynamic investigation of methanol and dimethyl ether synthesis from CO_2 hydrogenation, Korean J. Chem. Eng. 17 (2000) 210–216, https://doi.org/10.1007/BF02707145.

[65] C.V. Miguel, M.A. Soria, A. Mendes, L.M. Madeira, Direct CO_2 hydrogenation to methane or methanol from post-combustion exhaust streams – A thermodynamic study, J. Nat. Gas. Sci. Eng. 22 (2015) 1–8, https://doi.org/10.1016/j.jngse.2014.11.010.

[66] T.O. Bello, A.E. Bresciani, C.A.O. Nascimento, R.M.B. Alves, Thermodynamic analysis of carbon dioxide hydrogenation to formic acid and methanol, Chem. Eng. Sci. 242 (2021), 116731, https://doi.org/10.1016/j.ces.2021.116731.

[67] S. Kanuri, S. Roy, C. Chakraborty, S.P. Datta, S.A. Singh, S. Dinda, An insight of CO_2 hydrogenation to methanol synthesis: Thermodynamics, catalysts, operating

parameters, and reaction mechanism, Energ. Res. 46 (2022) 5503–5522, https://doi.org/10.1002/er.7562.

[68] C. Jia, J. Gao, Y. Dai, J. Zhang, Y. Yang, The thermodynamics analysis and experimental validation for complicated systems in CO_2 hydrogenation process, J. Energ. Chem. 25 (2016) 1027–1037, https://doi.org/10.1016/j.jechem.2016.10.003.

[69] X. He, CO_2 hydrogenation for ethanol production: a thermodynamic analysis, Int. J. Oil, Gas. Coal Eng. 5 (2017) 145–152, https://doi.org/10.11648/j.ogce.20170506.14.

[70] K. Stangeland, H. Li, Z. Yu, Thermodynamic analysis of chemical and phase equilibria in CO_2 hydrogenation to methanol, dimethyl ether, and higher alcohols, Ind. Eng. Chem. Res. 57 (2018) 4081–4094, https://doi.org/10.1021/acs.iecr.7b04866.

[71] S. Zhang, X. Liu, Z. Shao, H. Wang, Y. Sun, Direct CO_2 hydrogenation to ethanol over supported Co_2C catalysts: studies on support effects and mechanism, J. Catal. 382 (2020) 86–96, https://doi.org/10.1016/j.jcat.2019.11.038.

[72] H. Guo, S. Li, F. Peng, H. Zhang, L. Xiong, C. Huang, C. Wang, X. Chen, Roles investigation of promoters in K/Cu–Zn catalyst and higher alcohols synthesis from CO_2 hydrogenation over a novel two-stage bed catalyst combination system, Catal. Lett. 145 (2015) 620–630, https://doi.org/10.1007/s10562-014-1446-7.

[73] S. Li, H. Guo, C. Luo, H. Zhang, L. Xiong, X. Chen, L. Ma, Effect of iron promoter on structure and performance of K/Cu–Zn catalyst for higher alcohols synthesis from CO_2 hydrogenation, Catal. Lett. 143 (2013) 345–355, https://doi.org/10.1007/s10562-013-0977-7.

[74] P. Koukkari, R. Pajarre, A Gibbs energy minimization method for constrained and partial equilibria, Pure Appl. Chem. 83 (2011) 1243–1254, https://doi.org/10.1351/PAC-CON-10-09-36.

[75] H. Kusama, K. Okabe, K. Sayama, H. Arakawa, CO_2 hydrogenation to ethanol over promoted Rh/SiO_2 catalysts, Catal. Today 28 (1996) 261–266, https://doi.org/10.1016/0920-5861(95)00246-4.

[76] H. Kusama, K. Okabe, K. Sayama, H. Arakawa, Ethanol synthesis by catalytic hydrogenation of CO_2 over Rh-Fe/SiO_2 catalysts, Energy 22 (1997) 343–348, https://doi.org/10.1016/S0360-5442(96)00095-3.

[77] A. Goryachev, A. Pustovarenko, G. Shterk, N.S. Alhajri, A. Jamal, M. Albuali, L. van Koppen, I.S. Khan, A. Russkikh, A. Ramirez, T. Shoinkhorova, E.J. M. Hensen, J. Gascon, A multi-parametric catalyst screening for CO_2 hydrogenation to ethanol, ChemCatChem 13 (2021) 3324–3332, https://doi.org/10.1002/cctc.202100302.

[78] C. Yang, R. Mu, G. Wang, J. Song, H. Tian, Z.-J. Zhao, J. Gong, Hydroxyl-mediated ethanol selectivity of CO_2 hydrogenation, Chem. Sci. 10 (2019) 3161–3167, https://doi.org/10.1039/C8SC05608K.

[79] G.C. Bond, P.A. Sermon, G. Webb, D.A. Buchanan, P.B. Wells, Hydrogenation over supported gold catalysts, J. Chem. Soc., Chem. Commun. (1973) 444–445, https://doi.org/10.1039/C3973000444B.

[80] M. Haruta, Gold rush, Nature 437 (2005) 1098–1099, https://doi.org/10.1038/4371098a.

[81] G.J. Hutchings, Catalysis by gold, Catal. Today 100 (2005) 55–61, https://doi.org/10.1016/j.cattod.2004.12.016.

[82] A. Wittstock, V. Zielasek, J. Biener, C.M. Friend, M. Baumer, Nanoporous gold catalysts for selective gas-phase oxidative coupling of methanol at low temperature, Science 327 (2010) 319–322, https://doi.org/10.1126/science.1183591.

[83] L. Kesavan, R. Tiruvalam, M.H. Ab Rahim, M.I. Bin Saiman, D.I. Enache, R. L. Jenkins, N. Dimitratos, J.A. Lopez-Sanchez, S.H. Taylor, D.W. Knight, C. J. Kiely, G.J. Hutchings, Solvent-free oxidation of primary carbon-hydrogen bonds in toluene using Au-Pd alloy nanoparticles, Science 331 (2011) 195–199, https://doi.org/10.1126/science.1198458.

[84] Q.-Y. Bi, X.-L. Du, Y.-M. Liu, Y. Cao, H.-Y. He, K.-N. Fan, Efficient subnanometric gold-catalyzed hydrogen generation via formic acid decomposition under ambient conditions, J. Am. Chem. Soc. 134 (2012) 8926–8933, https://doi.org/10.1021/ja301696e.

[85] P. Johnston, N. Carthey, G.J. Hutchings, Discovery, development, and commercialization of gold catalysts for acetylene hydrochlorination, J. Am. Chem. Soc. 137 (2015) 14548–14557, https://doi.org/10.1021/jacs.5b07752.

[86] E. Monti, A. Ventimiglia, C.A.G. Soto, F. Martelli, E. Rodríguez-Aguado, J. A. Cecilia, P. Maireles-Torres, F. Ospitali, T. Tabanelli, S. Albonetti, F. Cavani, N. Dimitratos, Oxidative condensation/esterification of furfural with ethanol using preformed Au colloidal nanoparticles. Impact of stabilizer and heat treatment protocols on catalytic activity and stability, Mol. Catal. 528 (2022), 112438, https://doi.org/10.1016/j.mcat.2022.112438.

[87] S. Scurti, A. Allegri, F. Liuzzi, E. Rodríguez-Aguado, J.A. Cecilia, S. Albonetti, D. Caretti, N. Dimitratos, Temperature-dependent activity of gold nanocatalysts supported on activated carbon in redox catalytic reactions: 5-hydroxymethylfurfural oxidation and 4-nitrophenol reduction comparison, Catalysts 12 (2022) 323, https://doi.org/10.3390/catal12030323.

[88] E. Monti, A. Ventimiglia, C.A.G. Soto, F. Martelli, E. Rodríguez-Aguado, J. A. Cecilia, A. Sadier, F. Ospitali, T. Tabanelli, S. Albonetti, F. Cavani, R. Wojcieszak, N. Dimitratos, Effect of the colloidal preparation method for supported preformed colloidal Au nanoparticles for the liquid phase oxidation of 1,6-hexanediol to adipic acid, Catalysts 12 (2022) 196, https://doi.org/10.3390/catal12020196.

[89] D. Preti, C. Resta, S. Squarcialupi, G. Fachinetti, Carbon dioxide hydrogenation to formic acid by using a heterogeneous gold catalyst, Angew. Chem. Int. Ed. 50 (2011) 12551–12554, https://doi.org/10.1002/anie.201105481.

[90] A.A. Herzing, C.J. Kiely, A.F. Carley, P. Landon, G.J. Hutchings, Identification of active gold nanoclusters on iron oxide supports for CO oxidation, Science 321 (2008) 1331–1335, https://doi.org/10.1126/science.1159639.

[91] M. Turner, V.B. Golovko, O.P.H. Vaughan, P. Abdulkin, A. Berenguer-Murcia, M. S. Tikhov, B.F.G. Johnson, R.M. Lambert, Selective oxidation with dioxygen by gold nanoparticle catalysts derived from 55-atom clusters, Nature 454 (2008) 981–983, https://doi.org/10.1038/nature07194.

[92] S. Vajda, M.J. Pellin, J.P. Greeley, C.L. Marshall, L.A. Curtiss, G.A. Ballentine, J. W. Elam, S. Catillon-Mucherie, P.C. Redfern, F. Mehmood, P. Zapol, Subnanometre platinum clusters as highly active and selective catalysts for the oxidative dehydrogenation of propane, Nat. Mater. 8 (2009) 213–216, https://doi.org/10.1038/nmat2384.

[93] D. Wang, Q. Bi, G. Yin, W. Zhao, F. Huang, X. Xie, M. Jiang, Direct synthesis of ethanol via CO_2 hydrogenation using supported gold catalysts, Chem. Commun. 52 (2016) 14226–14229, https://doi.org/10.1039/C6CC08161D.

[94] D. Wang, Q. Bi, G. Yin, P. Wang, F. Huang, X. Xie, M. Jiang, Photochemical preparation of anatase titania supported gold catalyst for ethanol synthesis from CO_2 hydrogenation, Catal. Lett. 148 (2018) 11–22, https://doi.org/10.1007/s10562-017-2192-4.

[95] Z. He, Q. Qian, J. Ma, Q. Meng, H. Zhou, J. Song, Z. Liu, B. Han, Water-enhanced synthesis of higher alcohols from CO_2 hydrogenation over a Pt/Co_3O_4 catalyst under milder conditions, Angew. Chem., Int. Ed. 55 (2016) 737–741, https://doi.org/10.1002/anie.201507585.

[96] B. Ouyang, S. Xiong, Y. Zhang, B. Liu, J. Li, The study of morphology effect of Pt/Co_3O_4 catalysts for higher alcohol synthesis from CO_2 hydrogenation, Appl. Catal. A: Gen. 543 (2017) 189–195, https://doi.org/10.1016/j.apcata.2017.06.031.

[97] B. Qiao, A. Wang, X. Yang, L.F. Allard, Z. Jiang, Y. Cui, J. Liu, J. Li, T. Zhang, Single-atom catalysis of CO oxidation using Pt_1/FeO_x, Nat. Chem. 3 (2011) 634–641, https://doi.org/10.1038/nchem.1095.

[98] F.J. Caparrós, L. Soler, M.D. Rossell, I. Angurell, L. Piccolo, O. Rossell, J. Llorca, Remarkable carbon dioxide hydrogenation to ethanol on a palladium/iron oxide single-atom catalyst, ChemCatChem 10 (2018) 2365–2369, https://doi.org/10.1002/cctc.201800362.

[99] Y. Lou, F. Jiang, W. Zhu, L. Wang, T. Yao, S. Wang, B. Yang, B. Yang, Y. Zhu, X. Liu, CeO_2 supported Pd dimers boosting CO_2 hydrogenation to ethanol, Appl. Catal. B: Environ. 291 (2021), 120122, https://doi.org/10.1016/j.apcatb.2021.120122.

[100] X. Ye, C. Yang, X. Pan, J. Ma, Y. Zhang, Y. Ren, X. Liu, L. Li, Y. Huang, Highly Selective Hydrogenation of CO_2 to Ethanol via Designed Bifunctional Ir_1–In_2O_3 Single-Atom Catalyst, J. Am. Chem. Soc. 142 (2020) 19001–19005, https://doi.org/10.1021/jacs.0c08607.

[101] S.T. Yong, C.W. Ooi, S.P. Chai, X.S. Wu, Review of methanol reforming-Cu-based catalysts, surface reaction mechanisms, and reaction schemes, Int. J. Hydrog. Energ. 38 (2013) 9541–9552, https://doi.org/10.1016/j.ijhydene.2013.03.023.

[102] M. Takagawa, A. Okamoto, H. Fujimura, Y. Izawa, H. Arakawa, Ethanol synthesis from carbon dioxide and hydrogen, Stud. Surf. Sci. Catal. 114 (1998) 525–528, https://doi.org/10.1016/S0167-2991(98)80812-4.

[103] K. Higuchi, Y. Haneda, K. Tabata, Y. Nakahara, M. Takagawa, A study for the durability of catalysts in ethanol synthesis by hydrogenation of carbon dioxide, Stud. Surf. Sci. Catal. 114 (1998) 517–520, https://doi.org/10.1016/S0167-2991(98)80810-0.

[104] W. Guo, W.G. Gao, H. Wang, J.J. Tian, Higher alcohols synthesis from CO_2 hydrogenation over K_2O-modified $CuZnFeZrO_2$ catalysts, Adv. Mater. Res 827 (2014) 20–24, https://doi.org/10.4028/www.scientific.net/AMR.827.20.

[105] D. Xu, M. Ding, X. Hong, G. Liu, S.C.E. Tsang, Selective C_{2+} alcohol synthesis from direct CO_2 hydrogenation over a Cs-promoted Cu-Fe-Zn catalyst, ACS Catal. 10 (2020) 5250–5260, https://doi.org/10.1021/acscatal.0c01184.

[106] H.T. Luk, C. Mondelli, S. Mitchell, S. Siol, J.A. Stewart, D.C. Ferre, J. Perez-Ramirez, Role of carbonaceous supports and potassium promoter on higher alcohols synthesis over copper–iron catalysts, ACS Catal. 8 (2018) 9604–9618.

[107] M. Ding, J. Tu, M. Qiu, T. Wang, L. Ma, Y. Li, Impact of potassium promoter on Cu–Fe based mixed alcohols synthesis catalyst, Appl. Energ. 138 (2015) 584–589, https://doi.org/10.1016/j.apenergy.2014.01.010.

[108] D. Xu, M. Ding, X. Hong, G. Liu, Mechanistic aspects of the Role of K promotion on Cu−Fe-based catalysts for higher alcohol synthesis from CO_2 hydrogenation, ACS Catal. 10 (2020) 14516–14526, https://doi.org/10.1021/acscatal.0c03575.

[109] H.C. Woo, K.Y. Park, Y.G. Kim, I.S. Nam, J.S. Chung, J.S. Lee, Mixed alcohol synthesis from carbon monoxide and dihydrogen over potassium-promoted molybdenum carbide catalysts, Appl. Catal. 75 (1991) 267–280, https://doi.org/10.1016/S0166-9834(00)83136-X.

[110] J. Iranmahboob, D.O. Hill, H. Toghiani, K_2CO_3/Co-MoS_2/clay catalyst for synthesis of alcohol: influence of potassium and cobalt, Appl. Catal. A: Gen. 231 (2002) 99–108, https://doi.org/10.1016/S0926-860X(01)01011-0.

[111] Y. Yang, Y. Wang, S. Liu, Q. Song, Z. Xie, Z. Gao, Effect of lanthanum promotion on the unsupported Mo–Co–K sulfide catalysts for synthesis of mixed alcohols from syngas, Catal. Lett. 127 (2009) 448–455, https://doi.org/10.1007/s10562-008-9739-3.

[112] A.J.G. Da Silva, P. Claassens-Dekker, A.C.S. De Mattos Carvalho, A. M. Sanseverino, C.P.B. Quitete, A. Szklo, E.F. Sousa-Aguiar, Evaluation of MoS_2 based catalysts for the conversion of syngas into alcohols: a combinatorial approach, J. Environ. Chem. Eng. 2 (2014) 2148–2155, https://doi.org/10.1016/j.jece.2014.09.006.

[113] M.A. Kamorin, V.S. Dorokhov, E.A. Permyakov, O.L. Eliseev, A.L. Lapidus, V. M. Kogan, Comparative study of reduced and sulfide catalysts based on transition metals in conversion of CO and H_2, Kinet. Catal. 59 (2018) 311–319, https://doi.org/10.1134/S0023158418030084.

[114] K. Simeonov, J.H. Kim, D. Ferrari, D. Huelsman, G. Budroni, S. Corthals, Y. J. Pagan-Torres, CoMoS/K catalysts for higher alcohol synthesis from syngas prepared by mechano-chemical activation of molybdenite, Catal. Sci. Technol. 4 (2014) 922–924, https://doi.org/10.1039/C3CY00865G.

[115] X. Xi, F. Zeng, H. Cao, C. Cannilla, T. Bisswanger, S. de Graaf, Y. Pei, F. Frusteri, C. Stampfer, R. Palkovits, H.J. Heeres, Enhanced C_{3+} alcohol synthesis from syngas using $KCoMoS_x$ catalysts: effect of the Co-Mo ratio on catalyst performance, Appl. Catal. B: Environ. 272 (2020), 118950, https://doi.org/10.1016/j.apcatb.2020.118950.

[116] J.E. Hensley, S. Pylypenko, D.A. Ruddy, Deactivation and stability of K-$CoMoS_x$ mixed alcohol synthesis catalysts, J. Catal. 309 (2014) 199–208, https://doi.org/10.1016/j.jcat.2013.10.001.

[117] D.L.S. Nieskens, D. Ferrari, Y. Liu, R. Kolonko, The conversion of carbon dioxide and hydrogen into methanol and higher alcohols, Catal. Commun. 14 (2011) 111–113, https://doi.org/10.1016/j.catcom.2011.07.020.

[118] S. Liu, H. Zhou, L. Zhang, Z. Ma, Y. Wang, Activated carbon-supported Mo-Co-K sulfide catalysts for synthesizing higher alcohols from CO_2, Chem. Eng. Technol. 42 (2019) 962–970, https://doi.org/10.1002/ceat.201800401.

[119] Z. Gholami, Z. Tisler, V. Rubas, Recent advances in Fischer-Tropsch synthesis using cobalt-based catalysts: a review on supports, promoters, and reactors, Catal. Rev. 63 (2021) 512–595, https://doi.org/10.1080/01614940.2020.1762367.

[120] K. Jeske, A.C. Kizilkaya, I. Lopez-Luque, N. Pfander, M. Bartsch, P. Concepcion, G. Prieto, Design of cobalt fischer–tropsch catalysts for the combined production of liquid fuels and olefin chemicals from hydrogen-rich syngas, ACS Catal. 11 (2021) 4784–4798, https://doi.org/10.1021/acscatal.0c05027.

[121] M.K. Gnanamani, G. Jacobs, R.A. Keogh, W.D. Shafer, D.E. Sparks, S.D. Hopps, G. A. Thomas, B.H. Davis, Fischer-Tropsch synthesis: Effect of pretreatment conditions of cobalt on activity and selectivity for hydrogenation of carbon dioxide, Appl. Catal. A: Gen. 499 (2015) 39–46, https://doi.org/10.1016/j.apcata.2015.03.046.

[122] L. Wang, L. Wang, J. Zhang, X. Liu, H. Wang, W. Zhang, Q. Yang, J. Ma, X. Dong, S.J. Yoo, J.-G. Kim, X. Meng, F.-S. Xiao, Selective hydrogenation of CO_2 to ethanol over cobalt catalysts, Angew. Chem., Int. Ed. 57 (2018) 6104–6108, https://doi.org/10.1002/anie.201800729.

[123] L. Wang, S. He, L. Wang, Y. Lei, X. Meng, F.-S. Xiao, Cobalt−nickel catalysts for selective hydrogenation of carbon dioxide into ethanol, ACS Catal. 9 (2019) 11335–11340, https://doi.org/10.1021/acscatal.9b04187.

[124] A. Tsiotsias, B. Ehrhardt, B. Rudolph, L. Nodari, S. Kim, W. Jung, N.D. Charisiou, M.A. Goula, S. Mascotto, Bimetallic exsolved heterostructures of controlled composition with tunable catalytic properties, *ACS Nano* 16 (2022) 8904–8916, https://doi.org/10.1021/acsnano.1c11111.

[125] J. Wei, R. Yao, Q. Ge, D. Xu, C. Fang, J. Zhang, H. Xu, J. Sun, Precisely regulating Brønsted acid sites to promote the synthesis of light aromatics via CO_2 hydrogenation, Appl. Catal. B: Environ. 283 (2021), 119648, https://doi.org/10.1016/j.apcatb.2020.119648.

[126] C. Zhang, C. Cao, Y. Zhang, X. Liu, J. Xu, M. Zhu, W. Tu, Y.-F. Han, Unraveling the role of zinc on bimetallic Fe_5C_2–ZnO catalysts for highly selective carbon dioxide hydrogenation to high carbon α-olefins, ACS Catal. 11 (2021) 2121–2133, https://doi.org/10.1021/acscatal.0c04627.

[127] R. Yao, J. Wei, Q. Ge, J. Xu, Y. Han, Q. Ma, H. Xu, J. Sun, Monometallic iron catalysts with synergistic Na and S for higher alcohols synthesis via CO_2 hydrogenation, Appl. Catal. B: Environ. 298 (2021), 120556, https://doi.org/10.1016/j.apcatb.2021.120556.

[128] L.B. Hoch, T.E. Wood, P.G. O'Brien, K. Liao, L.M. Reyes, C.A. Mims, G.A. Ozin, The rational design of a single-component photocatalyst for gas-phase CO_2 reduction using Both UV and visible light, Adv. Sci. 1 (2014) 1400013, https://doi.org/10.1002/advs.201400013.

[129] Z.M. Detweiler, J.L. White, S.L. Bernasek, A.B. Bocarsly, Anodized indium metal electrodes for enhanced carbon dioxide reduction in aqueous electrolyte, Langmuir 30 (2014) 7593–7600, https://doi.org/10.1021/la501245p.

[130] P. Brandao, A.J. Burke, M. Pineiro, A decade of Indium-catalyzed multicomponent reactions (MCRs), Eur. J. Org. Chem. 2020 (2020) 5501–5513, https://doi.org/10.1002/ejoc.202000596.

[131] J. Ye, C. Liu, Q. Ge, DFT study of CO_2 adsorption and hydrogenation on the In_2O_3 surface, J. Phys. Chem. C. 116 (2012) 7817–7825, https://doi.org/10.1021/jp3004773.

[132] J. Ye, C. Liu, D. Mei, Q. Ge, Active oxygen vacancy site for methanol synthesis from CO_2 hydrogenation on In_2O_3(110): a DFT study, ACS Catal. 3 (2013) 1296–1306, https://doi.org/10.1021/cs400132a.

[133] K. Sun, Z. Fan, J. Ye, J. Yan, Q. Ge, Y. Li, W. He, W. Yang, C.-J. Liu, Hydrogenation of CO_2 to methanol over In_2O_3 catalyst, J. CO_2 Util. 12 (2015) 1–6, https://doi.org/10.1016/j.jcou.2015.09.002.

[134] O. Martin, A.J. Martin, C. Mondelli, S. Mitchell, T.F. Segawa, R. Hauert, C. Drouilly, D. Curulla-Ferre, J. Perez-Ramirez, Indium oxide as a superior catalyst for methanol synthesis by CO_2 hydrogenation, Angew. Chem., Int. Ed. 55 (2016) 6261–6265, https://doi.org/10.1002/anie.201600943.

[135] X. Jiang, X. Nie, X. Guo, C. Song, J.G. Chen, Recent advances in carbon dioxide hydrogenation to methanol via heterogeneous catalysis, Chem. Rev. 120 (2020) 7984–8034, https://doi.org/10.1021/acs.chemrev.9b00723.

[136] J. Zhong, X. Yang, Z. Wu, B. Liang, Y. Huang, T. Zhang, State of the art and perspectives in heterogeneous catalysis of CO_2 hydrogenation to methanol, Chem. Soc. Rev. 49 (2020) 1385–1413, https://doi.org/10.1039/C9CS00614A.

[137] Z. Zhou, P. Gao, Direct carbon dioxide hydrogenation to produce bulk chemicals and liquid fuels via heterogeneous catalysis, Chin. J. Catal. 43 (2022) 2045–2056, https://doi.org/10.1016/S1872-2067(22)64107-X.

[138] A. Tsoukalou, A.I. Serykh, E. Willinger, A. Kierzkowska, P.M. Abdala, A. Fedorov, C.R. Müller, Hydrogen dissociation sites on indium-based ZrO_2-supported catalysts for hydrogenation of CO_2 to methanol, Catal. Today 387 (2022) 38–46, https://doi.org/10.1016/j.cattod.2021.04.010.

[139] C.-Y. Chou, R.F. Lobo, Direct conversion of CO_2 into methanol over promoted indium oxide-based catalysts, Appl. Catal. A: Gen. 583 (2019), 117144, https://doi.org/10.1016/j.apcata.2019.117144.

[140] P. Gao, S. Li, X. Bu, S. Dang, Z. Liu, H. Wang, L. Zhong, M. Qiu, C. Yang, J. Cai, W. Wei, Y. Sun, Direct conversion of CO_2 into liquid fuels with high selectivity over a bifunctional catalyst, Nat. Chem. 9 (2017) 1019–1024, https://doi.org/10.1038/nchem.2794.

[141] T. Witoon, T. Numpilai, Nijpanich Su, N. Chanlek, P. Kidkhunthod, C.K. Cheng, K. H. Ng, D.-V.N. Vo, S. Ittisanronnachai, C. Wattanakit, M. Chareonpanich, J. Limtrakul, Enhanced CO_2 hydrogenation to higher alcohols over K-Co promoted In_2O_3 catalysts, Chem. Eng. J. 431 (2022), 133211, https://doi.org/10.1016/j.cej.2021.133211.

[142] M.K. Gnanamani, G. Jacobs, H.H. Hamdeh, W.D. Shafer, F. Liu, S.D. Hopps, G. A. Thomas, B.H. Davis, Hydrogenation of carbon dioxide over Co–Fe bimetallic catalysts, ACS Catal. 6 (2016) 913–927, https://doi.org/10.1021/acscatal.5b01346.

[143] M.K. Gnanamani, H.H. Hamdeh, G. Jacobs, W.D. Shafer, S.D. Hopps, A.T. Gerald, H.D. Burtron, Hydrogenation of carbon dioxide over K-promoted FeCo bimetallic catalysts prepared from mixed metal oxalates, ChemCatChem 9 (2017) 1303–1312, https://doi.org/10.1002/cctc.201601337.

[144] X. Xi, F. Zeng, H. Zhang, X. Wu, J. Ren, T. Bisswanger, C. Stampfer, J.P. Hofmann, R. Palkovits, H.J. Heeres, CO_2 hydrogenation to higher alcohols over K-promoted bimetallic Fe−In catalysts on a Ce−ZrO_2 support, ACS Sust. Chem. Eng. 9 (2021) 6235–6249, https://doi.org/10.1021/acssuschemeng.0c08760.

[145] N.D. Charisiou, G. Siakavelas, L. Tzounis, V. Sebastian, A. Monzon, M.A. Baker, S. J. Hinder, K. Polychronopoulou, I.V. Yentekakis, M.A. Goula, An in depth investigation of deactivation through carbon formation during the biogas dry reforming reaction for Ni supported on modified with CeO_2 and La_2O_3 zirconia catalysts. Int. J. Hydrog. Energ. 43 (2018) 18955–18976, https://doi.org/10.1016/j.ijhydene.2018.08.074.

[146] M.A. Goula, N.D. Charisiou, G. Siakavelas, L. Tzounis, I. Tsiaoussis, P. Panagiotopoulou, G. Goula, I.V. Yentekakis, Syngas production via the biogas dry reforming reaction over Ni supported on zirconia modified with CeO_2 or La_2O_3 catalysts, Int. J. Hydrog. Energ. 42 (2017) 13724–13740, https://doi.org/10.1016/j.ijhydene.2016.11.196.

[147] Z. He, Q. Qian, Z. Zhang, Q. Meng, H. Zhou, Z. Jiang, B. Han, Synthesis of higher alcohols from CO_2 hydrogenation over a PtRu/Fe_2O_3 catalyst under supercritical condition, Philos. Trans. R. Soc. A. 373 (2015) 0006, https://doi.org/10.1098/rsta.2015.0006.

[148] S. Bai, Q. Shao, P. Wang, Q. Dai, X. Wang, X. Huang, Highly active and selective hydrogenation of CO_2 to ethanol by ordered Pd–Cu nanoparticles, 6827–2830, J. Am. Chem. Soc. 139 (2017), https://doi.org/10.1021/jacs.7b03101.

[149] J.-C. Li, Y. Cao, S. Xu, P. He, L. Wang, X. Hui, H.-Q. Li, Catalytic hydrogenation of CO_2 to produce lower alcohols and ether over Co-Cu-Zn-Al catalyst, Greenh. Gases 11 (2021) 1180–1190, https://doi.org/10.1002/ghg.2135.

[150] O.M. Yaghi, D.A. Richardson, G. Li, C.E. Davis, T.L. Groy, Open-framework solids with diamond-like structures prepared from clusters and metal-organic building blocks, MRS Proc. 371 (1994) 15, https://doi.org/10.1557/PROC-371-15.

[151] A.G. Georgiadis, N.D. Charisiou, I.V. Yentekakis, M.A. Goula, Hydrogen sulfide (H_2S) removal via MOFs, Materials 13 (2020) 3640, https://doi.org/10.3390/ma13163640.

[152] A. Bavykina, N. Kolobov, I.S. Khan, J.A. Bau, A. Ramirez, J. Gascon, Metal–organic frameworks in heterogeneous catalysis: recent progress, new trends, and future perspectives, Chem. Rev. 120 (2020) 8468–8535, https://doi.org/10.1021/acs.chemrev.9b00685.

[153] B. An, Z. Li, Y. Song, J. Zhang, L. Zeng, C. Wang, W. Lin, Cooperative copper centres in a metal–organic framework for selective conversion of CO_2 to ethanol, Nat. Catal. 2 (2019) 709–717, https://doi.org/10.1038/s41929-019-0308-5.

[154] A. Tsiotsias, N.D. Charisiou, A. AlKhoori, S. Gaber, V. Sebastian, S.J. Hinder, M. A. Baker, K. Polychronopoulou, M.A. Goula, Towards maximizing conversion of ethane and carbon dioxide into synthesis gas using highly stable Ni-perovskite catalysts, *J. CO_2 Util.* 61 (2022), 102046, https://doi.org/10.1016/j.jcou.2022.102046.

[155] J.-N. Zheng, K. An, J.-M. Wang, J. Li, Y. Liu, Direct synthesis of ethanol via CO_2 hydrogenation over the Co/La-Ga-O composite oxide catalyst, J. Fuel Chem. Technol. 47 (2019) 697–708, https://doi.org/10.1016/S1872-5813(19)30031-3.

[156] K. An, S. Zhang, J. Wang, Q. Liu, Z. Zhang, Y. Liu, A highly selective catalyst of Co/$La_4Ga_2O_9$ for CO_2 hydrogenation to ethanol, J. Energ. Chem. 56 (2021) 486–495, https://doi.org/10.1016/j.jechem.2020.08.045.

[157] J. Liang, Z. Liang, R. Zou, Y. Zhao, Heterogeneous catalysis in zeolites, mesoporous silica, and metal–organic frameworks, Adv. Mater. 29 (2017) 1701139, https://doi.org/10.1002/adma.201701139.

[158] G. Aguirre-Cruz, F. Legorreta-Garcia, G. Aguirre-Cruz, L. Stanciu, G. Aguirre-Alvarez, Synthesis of hierarchical silica zeolites for heterogenous catalysis and adsorption, Micro Mesoporous Mater. 345 (2022), 112274, https://doi.org/10.1016/j.micromeso.2022.112274.

[159] L. Ding, T. Shi, J. Gu, Y. Cui, Z. Zhang, C. Yang, T. Chen, M. Lin, P. Wang, N. Xue, L. Peng, X. Guo, Y. Zhu, Z. Chen, W. Ding, CO_2 hydrogenation to ethanol over Cu@Na-Beta, Chem 6 (2020) 2673–2689, https://doi.org/10.1016/j.chempr.2020.07.001.

[160] C. Yang, S. Liu, Y. Wang, J. Song, G. Wang, S. Wang, Z.-J. Zhao, R. Mu, J. Gong, The interplay between structure and product selectivity of CO_2 hydrogenation,

Angew. Chem., Int. Ed. 58 (2019) 11242–11247, https://doi.org/10.1002/anie.201904649.

[161] D. Xu, H. Yang, X. Hong, G. Liu, S.C.E. Tsang, Tandem catalysis of direct CO_2 hydrogenation to higher alcohols, ACS Catal. 11 (2021) 8978–8984, https://doi.org/10.1021/acscatal.1c01610.

[162] Y. Wang, K. Wang, B. Zhang, X. Peng, X. Gao, G. Yang, H. Hu, M. Wu, N. Tsubaki, Direct conversion of CO_2 to ethanol boosted by intimacy-sensitive multifunctional catalysts, ACS Catal. 11 (2021) 11742–11753, https://doi.org/10.1021/acscatal.1c01504.

[163] Y. Wang, D. Xu, X. Zhang, X. Hong, G. Liu, Selective C_{2+} alcohol synthesis by CO_2 hydrogenation via a reaction-coupling strategy, Catal. Sci. Technol. 12 (2022) 1539–1550, https://doi.org/10.1039/D1CY02196F.

[164] D.E. Fogg, E.N. dos Santos, Tandem catalysis: a taxonomy and illustrative review, Coord. Chem. Rev. 248 (2004) 2365–2379, https://doi.org/10.1016/j.ccr.2004.05.012.

[165] M.R. Rahimpour, A dual-catalyst bed concept for industrial methanol synthesis, Chem. Eng. Commun. 194 (2007) 1638–1653, https://doi.org/10.1080/00986440701446227.

[166] M.R. Rahimpour, A two-stage catalyst bed concept for conversion of carbon dioxide into methanol, Fuel Proc. Technol. 89 (2008) 556–566, https://doi.org/10.1016/j.fuproc.2007.10.011.